Monitoring Cointegration in Systems of Cointegrating Relationships

This version: December 20, 2022

Etienne Theising[1] & Dominik Wied

Institute of Econometrics and Statistics
University of Cologne

Abstract

Monitoring statistics for structural changes in systems of cointegrating relationships are proposed. The approach is based on parameter estimation over a calibration period. In case of homogenous systems and cross-sectional independence the pooled fully modified OLS estimator takes into account the effects of error serial correlation and regressor endogeneity. Cross-sectional dependence is allowed by using the pooled fully modified GLS estimator for homogenous systems and the fully modified SUR estimator for inhomogenous systems. The detectors show decent behaviour under the null hypothesis with controlled rejection probabilities and power against two alternatives for different data generating processes. An empirical application investigates deviations from the arbitrage parity condition for exchange rate triplets including Bitcoin. The procedures detect breakpoints in May to August 2014 and in January to May 2015 indicating an instability in arbitrage parities. Following this, a promising portfolio trading strategy based on the breakdates is constructed.

Keywords: Bitcoin, Hypothesis Testing, Monitoring, System Cointegration, Triangular Arbitrage Parity

MSC Codes: 62F03, 62H15, 62M10, 62P20

JEL Codes: C12, C33, G14

---

[1]Correspondence to: University of Cologne, Institute of Econometrics and Statistics, Albertus Magnus Platz, 50923 Cologne, Germany. E-mail address: e.theising@uni-koeln.de (E. Theising).

1. Introduction

This paper proposes residual based self-normalized monitoring procedures for structural change in a system of homogeneous cointegrating regressions. Such procedures might be useful to detect deviations from stable economic relationships, e.g. macroeconomic equations for housing prices or financial equations for exchange rates. There is recent empirical evidence that such relationships might collapse (Anundsen, 2015, for the subprime bubble, Reynolds et al., 2021, and Reynolds et al., 2018, for cryptocurrencies) and we provide a methodological contribution to formally detect such collapses as early as possible. This is relevant from an economic point of view, but also for potential subsequent econometric analyses (see, e.g., Arsova and Örsal, 2021). As we assume that N is small and T is large, our procedure is typically most relevant for financial data.

Our asymptotically valid panel data method is an extension of the single equation monitoring procedure of Wagner and Wied (2017). Specifically, on the one hand, we assume homogeneous parameters and cross-sectional independent and identically distributed errors. On the other hand, we discuss extensions to the cases of heterogenous parameters and cross-sectional dependence. Our procedures are consistent if the cointegrating relationship turn to a spurious regression or if there is a break in the trend and/or slope parameters. The date of the potential change points does not need to be known a priori. Our monitoring procedures require parameter estimates and a monitoring statistic. We follow the ideas of Chu et al. (1996) and base the parameter estimates on a break-free (or assumed to be break-free) calibration period as a fraction of the whole sample size. The monitoring procedures use residuals calculated from these parameter estimates to calculate cointegration test statistics over expanding windows. Since the limiting distributions of our test statistics depend on the fraction of the calibration period, we in fact propose "closed-end" monitoring procedures, i.e. the monitoring horizon has to be specified beforehand.

We use the pooled fully modified OLS (PFM-OLS) estimator by Phillips and Moon (1999) to obtain nuisance parameter free null limiting distributions of the monitoring statistics and a pooled fully modified feasible GLS (PFM-GLS) estimator as well as the fully modified SUR (FM-SUR) estimator by Moon (1999) in case of cross-sectionally dependent cointegrating regressions. The limiting distributions also depend on the choice of deterministic regressors as well as the number of I(1)-regressors. Our monitoring statistics are based on the properly scaled partial sum process of FM-OLS-type residuals and inspired by the statistics in Wagner and Wied (2017) which are based on the statistic

of the Shin (1994) test. We analyze our approach with respect to different transformations from a multivariate partial sum process to a scalar test statistic.

A simulation study assesses the performance of the PFM-OLS procedure in terms of rejection probabilities under the null hypothesis as well as power and detection delays under various alternatives, including influence of regressor endogeneity and serial correlation, sample size and fraction of the calibration period m. Under the null hypothesis the procedures work well in terms of null rejection probabilities close to the chosen significance level. We further investigate how the PFM-GLS and FM-SUR procedures work under cross-sectional dependence assumptions. For a variety of alternatives we investigate both power and detection times, which serve as natural estimates of potential breakpoints. Finally, we provide simulations which indicate that, in terms of null rejection probabilities, one is advised to choose a monitoring period as long as possible such that the calibration period is as little a fraction of the whole period as possible.

We provide a test for stability in bivariate systems of homogeneous cointegrating relationships in triangular arbitrage parities for logarithmic exchange rate triplets including Bitcoin as an illustrative application example. We apply the procedures to a stochastic variant of the aforementioned parity arising from no-arbitrage assumptions between triplets of currency exchange rates such that there is no profit in instantaneous circular transactions. We assume that violations of triangular arbitrage parities under normal market conditions are stationary and a turn to non-stationary deviations is a sign of mispricing not due to financial frictions – also referred to as financial market dislocation. Reynolds et al. (2021) find empirical evidence of such mispricing in currency triplets including Bitcoin using the Wagner and Wied (2017) monitoring for single equation cointegrating relationships and use their results for a currency portfolio strategy. Our sample ranges from 1 May 2013 until 31 December 2015, with the calibration period ranging until 8 November 2013, assuming a break free calibration period due to stable Bitcoin prices. The monitoring statistics indicate structural change in May to August 2014 and in January to May 2015 for some pairs of exchange rate triplets. Important dates during monitoring and prior to the detected breaks are the ending of the cap on euro-swiss franc exchange rates by the Swiss National Bank in January 2015 and, in February 2014, the closing of Mt. Gox, a Japanese Bitcoin exchange where 70% of all tradings took place up to its closing (Decker and Wattenhofer, 2014), which in turn resulted in the loss of $850,000$ Bitcoin with a total value of 473 million USD at that time (Fink and Johann, 2014). Reynolds et al. (2021) do not account for testing several cointegrating relationships at a time, in contrast, these monitoring procedures do. We

apply our results to construct a portfolio trading strategy using the detected breaks as a sign of currency market instabilities.

The paper is organized as follows: Section 2 presents the model, the assumptions as well as the monitoring statistics. Section 3 presents the results from the simulation study, whilst Section 4 is dedicated to the application. Section 5 briefly summarizes and concludes. Three appendices follow the main text: Appendix A contains all proofs, Appendix B describes the simulation of critical values and Appendix C shows additional results on error covariances of the application and selected simulation cases.

2. Monitoring Systems of Cointegrating Regressions

We consider monitoring a potential structural change in a system of N cointegrating relationships (which we refer to as cointegrating regressions or cointegrating equations)

$$y_{n,t} = \begin{cases} D_t'\theta_{D,n} + X_{n,t}'\theta_{X,n} + u_{n,t} & , t = 1, \ldots, [rT], \\ D_t'\theta_{D,1,n} + X_{n,t}'\theta_{X,1,n} + u_{n,t} & , t = [rT] + 1, \ldots, T, \end{cases} \tag{1}$$

and

$$\Delta X_{n,t} = v_{n,t}, \quad t = 1, \ldots, T, \tag{2}$$

for $n = 1, \ldots, N$. Throughout the paper, we assume a break-free calibration period of length $[mT]$ at the sample beginning and consider the case of small N and large T, i.e. for asymptotics, N is fixed and $T \to \infty$. $y_{n,t}$ is scalar, $D_t \in \mathbb{R}^p$ is the deterministic trend function, $X_{n,t}$ is a non-cointegrated k-dimensional random vector of I(1) regressors, $u_{n,t}$ is a zero mean error process and $0 < m \le r < 1$. We allow for endogenous regressors and serial correlation in the zero mean errors $v_{n,t} = [v_{n,t,1}, \ldots, v_{n,t,k}]'$ of $X_{n,t}$ as well as correlation across k and n. Let $\theta_n = [\theta_{D,n}', \theta_{X,n}]'$ and $\theta_{1,n} = [\theta_{D,1,n}', \theta_{X,1,n}]'$.

We test the following pair of hypotheses:

$$H_0 : \begin{cases} \theta_n = \theta_{1,n} \text{ for all } m \le r < 1, n = 1, \ldots, N, \text{ and} \\ \{u_{n,t}\}_{t=1,\ldots,T} \text{ is I(0) for all } n = 1, \ldots, N \end{cases} \tag{3}$$

and

$$H_1 : \begin{cases} \theta_n \neq \theta_{1,n} \text{ for some } m \le r < 1, n \in \{1, \ldots, N\} \textbf{ or} \\ \{u_{n,t}\}_{t=1,\ldots,[rT]} \text{ is I(0) and } \{u_{n,t}\}_{t=[rT]+1,\ldots,T} \text{ is I(1)} \\ \text{for some } m \le r < 1, n \in \{1, \ldots, N\} \end{cases} \tag{4}$$
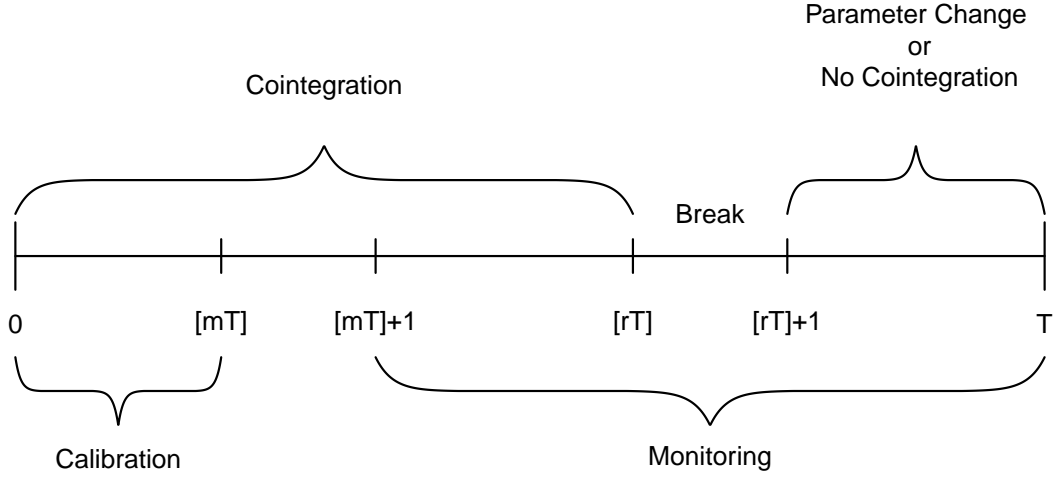
Figure 1: Own illustration of the monitoring procedure

Under the null hypothesis no structural change occurs, i.e. $\theta_{D,n} = \theta_{D,1,n}$ and $\theta_{X,n} = \theta_{X,1,n}$ and $\{u_{n,t}\}_{t=1,\dots,T}$ is I(0) for all $n = 1,\dots,N$. Under the alternative there is either a change in the parameter or a turn from cointegrating to spurious regression in at least one cointegrating relationship at a sample fraction $[rT]$ greater or equal to $[mT]$ and our procedures test for all potential breakpoints uniformly. A crucial question is how to choose m in practice. The decision might be based on economic arguments and it is possible to support such a choice with a retrospective panel cointegration test as reviewed in Breitung and Pesaran (2008). Our simulations (Figures 4 and 5) indicate that m should be rather small to have good size properties and it might be good practice to choose a fraction of 1/10 such as 0.2 or 0.3.

Regarding the trend function we impose the following assumption:

Assumption 1. *There exists a sequence of $p \times p$ scaling matrices $G_{D,T} > 0$, satisfying $||G_{D,T}|| \to 0$ for $T \to \infty$ ($||\cdot||$ any matrix norm), and a p-dimensional vector of functions $D(z)$ with $0 < \int_0^s D(z)D(z)' \mathrm{d}z < \infty$ for $0 \le s \le 1$, such that*

$$\lim_{T \to \infty} \sup_{0 \le s \le 1} \left|\left| T^{1/2} G_{D,T} D_{[sT]} - D(s) \right|\right|_2 = 0 \tag{5}$$

for $||\cdot||_2$ the Euclidean norm.

This assumption is essentially the same as in Phillips and Hansen (1990, p. 102)

and ensures a well defined limit of the scaled deterministic regressors. In case of a polynomial trend $D_t = [1, t, t^2, \ldots, t^{p-1}]'$ the assumption is satisfied by $G_{D,T} = \text{diag}\left(T^{-1/2}, T^{-1}, \ldots, T^{-p/2}\right)$ and $D(s) = [1, s, s^2, \ldots, s^{p-1}]'$.

Let $\eta_t := [u_t', v_t]'$ be the stacked errors with $u_t = [u_{1,t}, \ldots, u_{N,t}]'$ and $v_t = [v_{1,t}', \ldots, v_{N,t}']'$. Regarding the error process $\{\eta_t\}$ we assume that a functional central limit theorem holds:

Assumption 2.
(a): The stationary process $\{\eta_t\}$ fulfills

$$T^{-1/2} \sum_{t=1}^{[sT]} \eta_t = T^{-1/2} \sum_{t=1}^{[sT]} \begin{bmatrix} u_t \\ v_t \end{bmatrix} \Rightarrow B(s) := BM(\Omega) = \Omega^{1/2} W(s) \tag{6}$$

with $W(s) = [W_{u \cdot v}(s)', W_v(s)']'$ an $N(k+1)$-dimensional vector of standard Brownian motions and $0 < \Omega < \infty$, where

$$\Omega = \begin{bmatrix} \Omega_{uu} & \Omega_{uv} \\ \Omega_{vu} & \Omega_{vv} \end{bmatrix} := \sum_{h=-\infty}^{\infty} \mathbb{E}(\eta_0 \eta_h'). \tag{7}$$

(b): Denoting $S_t^{\eta} := \sum_{j=1}^{t} \eta_j$ it holds that

$$T^{-1} \sum_{t=1}^{[sT]} S_t^{\eta} \eta_t' \Rightarrow \int_0^s B(r) \mathrm{d}B(r)' + \Delta \tag{8}$$

with $\Delta := \sum_{h=0}^{\infty} \mathbb{E}(\eta_0 \eta_h')$.

(c): (a) and (b) hold jointly.

$W_{u \cdot v}(s) = [W_{u \cdot v, 1}(s), \ldots, W_{u \cdot v, N}(s)]'$ is an N-dimensional vector of standard Brownian motions and $W_v(s) = [W_{v,1}(s)', \ldots, W_{v,N}(s)']'$ consists of N different k-dimensional vectors of standard Brownian motions. We partition $B(s) = [B_u(s)', B_v(s)']'$, where $B_v(s) = [B_{v,1}(s)', \ldots, B_{v,N}(s)']'$ and $B_{v,n}(s)$ is a k-dimensional vector of Gaussian processes for $n = 1, \ldots, N$. The decomposition $B(s) = \Omega^{1/2} W(s)$ holds with

$$\Omega^{1/2} := \begin{pmatrix} (\Omega_{uu} - \Omega_{uv} \Omega_{vv}^{-1} \Omega_{vu})^{1/2} & \Omega_{uv} \Omega_{vv}^{-1/2} \\ \mathbf{0}_{kN \times N} & \Omega_{vv}^{1/2} \end{pmatrix}, \tag{9}$$

where $\mathbf{0}_{kN \times N}$ is a kN by N matrix of zeros. The assumption $\Omega_{vv} > 0$ excludes cointegration among the regressors X_t which is typically assumed for FM-OLS estimation.

We detail our notion of I(0) and I(1) processes and call a univariate stochastic process $\{\xi_t\}_{t \in \mathbb{Z}}$ I(0) if it fullfills (potentially after demeaning) a functional central limit theorem, i.e. if it holds for $0 \leq s \leq 1$ that $T^{-1/2} \sum_{t=1}^{[sT]} \xi_t \Rightarrow \omega W(s)$, where $W(s)$ denotes a standard Brownian motion and $0 < \omega < \infty$ is the long-run varaince $\omega^2 := \sum_{t=-\infty}^{\infty} \mathbb{E}(\xi_0 \xi_t)$ of $\{\xi_t\}_{t \in \mathbb{Z}}$. Therefore, an I(1) process $\{\zeta_t\}_{t \in \mathbb{Z}}$ with $\zeta_t - \zeta_{t-1} = \xi_t$, i.e. a summed up I(0) process, fulfills $T^{-1/2} \zeta_{[sT]} \Rightarrow \omega W(s)$ for all $0 \leq s \leq 1$ and ω and $W(s)$ as above.

The monitoring procedures are based on consistent estimators of the parameter vectors θ_n and (co-)variance parameters. Similar to Chu et al. (1996) we allow structural change only after a break-free calibration period of size $[mT]$ ($0 < m < 1$) at the beginning of the monitoring in all N cointegrating regressions (c.f. Figure 1). We obtain residuals via an estimator $\hat{\theta}_m$ of the fully modified type, which has been studied in detail with regards to panel data structures, based on the calibration period and the corresponding N-dimensional residuals $\hat{u}_{t;m}^+$. The monitoring procedure evaluates whether the properly scaled partial sum process of these residuals

$$T^{-1/2} \sum_{t=1}^{[sT]} \hat{u}_{t;m}^+ \tag{10}$$

becomes "too large". In view of Assumption 2, the partial sum process (10) serves as a natural basis for our monitoring procedure. We show that (10) converges to a mixture of Gaussian processes with nuisance parameters. The number of nuisance parameters and the precise limiting distribution depend on the set of considered assumptions. Further, the limiting distribution depends on m, the deterministic trend D_t and the number of regressors k as well.

The bases of scalar test statistics are three detectors constructed by different real-valued transformations of the N-dimensional residual process, i.e. mappings: $\mathbb{R}^N \to \mathbb{R}$, and we derive their asymptotic behaviour. The detectors are

$$\hat{H}_1^{m,+}(s) := \frac{\left\|T^{-1/2} \sum_{t=[mT]+1}^{[sT]} \hat{u}_{t;m}^+\right\|_2^2}{\left\|T^{-1/2} \sum_{t=1}^{[mT]} \hat{u}_{t;m}^+\right\|_2^2} = \frac{\sum_{n=1}^{N} \left(T^{-1/2} \sum_{t=[mT]+1}^{[sT]} \hat{u}_{n,t;m}^+\right)^2}{\sum_{n=1}^{N} \left(T^{-1/2} \sum_{t=1}^{[mT]} \hat{u}_{n,t;m}^+\right)^2}, \tag{11}$$

$$\hat{H}_2^{m,+}(s) := \frac{T^{-1}\sum_{i=[mT]+1}^{[sT]}\left\|T^{-1/2}\sum_{t=1}^{i}\hat{u}_{t;m}^{+}\right\|_2^2}{T^{-1}\sum_{i=1}^{[mT]}\left\|T^{-1/2}\sum_{t=1}^{i}\hat{u}_{t;m}^{+}\right\|_2^2}$$

$$= \frac{\sum_{n=1}^{N}T^{-1}\sum_{i=[mT]+1}^{[sT]}\left(T^{-1/2}\sum_{t=1}^{i}\hat{u}_{n,t;m}^{+}\right)^2}{\sum_{n=1}^{N}T^{-1}\sum_{i=1}^{[mT]}\left(T^{-1/2}\sum_{t=1}^{i}\hat{u}_{n,t;m}^{+}\right)^2} \tag{12}$$

and

$$\hat{H}_3^{m,+}(s) := \frac{\left\|T^{-1}\sum_{i=[mT]+1}^{[sT]}T^{-1/2}\sum_{t=1}^{i}\hat{u}_{t;m}^{+}\right\|_2^2}{\left\|T^{-1}\sum_{i=1}^{[mT]}T^{-1/2}\sum_{t=1}^{i}\hat{u}_{t;m}^{+}\right\|_2^2}$$

$$= \frac{\sum_{n=1}^{N}\left(T^{-1}\sum_{i=[mT]+1}^{[sT]}T^{-1/2}\sum_{t=1}^{i}\hat{u}_{n,t;m}^{+}\right)^2}{\sum_{n=1}^{N}\left(T^{-1}\sum_{i=1}^{[mT]}T^{-1/2}\sum_{t=1}^{i}\hat{u}_{n,t;m}^{+}\right)^2}, \tag{13}$$

with $\hat{u}_{t;m}^{+} = [\hat{u}_{1,t;m}^{+},\ldots,\hat{u}_{N,t;m}^{+}]$. Clearly, the numerator in (12) turns into the detector used by Wagner and Wied (2017) by setting $n = 1$ and into the Shin (1994) statistic by additionally setting $m = 0$ and $s = 1$.

In the following Sections 2.1 – 2.3 we derive the limiting distribution $\mathbf{W}_{\mathbf{u}\cdot\mathbf{v}}(s)$ of the partial sum process (10), such that

$$\frac{1}{\sqrt{T}}\sum_{t=1}^{[sT]}\hat{u}_{t;m}^{+} \Rightarrow \mathbf{W}_{\mathbf{u}\cdot\mathbf{v}}(s), \tag{14}$$

where $\mathbf{W}_{\mathbf{u}\cdot\mathbf{v}}(s) = [\mathbf{W}_{\mathbf{u}\cdot\mathbf{v},\mathbf{1}},\ldots,\mathbf{W}_{\mathbf{u}\cdot\mathbf{v},\mathbf{N}}]'$ is a functional of Brownian motions and depends on the set of assumptions specified in the respective Sections. All detectors are continuous mappings of the scaled partial sum process (10) and we use (14) along with the continuous mapping theorem to construct statistical hypothesis tests by the following Lemma 1 which is valid for three sets of assumptions and refers to three different convergence results for (14), Lemma 3 in Section 2.1 for cross-sectional independence, Lemma 5 in Section 2.2 for homogeneity and cross-sectional dependence and Lemma 7 in Section 2.3 for heterogeneity and cross-sectional dependence.

Lemma 1. *Let the assumptions of Lemma 3, 5 or 7 be in place, respectively, and let N be fixed. Then it holds that*

$$\hat{H}_1^{m,+}(s) \Rightarrow \frac{\sum_{n=1}^{N}\left(\mathbf{W}_{\mathbf{u}\cdot\mathbf{v},\mathbf{n}}(s) - \mathbf{W}_{\mathbf{u}\cdot\mathbf{v},\mathbf{n}}(m)\right)^2}{\sum_{n=1}^{N}\mathbf{W}_{\mathbf{u}\cdot\mathbf{v},\mathbf{n}}(m)^2} \qquad =: \mathcal{H}_1^{m,+}(s), \tag{15}$$

$$\hat{H}_2^{m,+}(s) \Rightarrow \frac{\sum_{n=1}^N \int_m^s \left(\mathbf{W_{u\cdot v,n}}(t)\right)^2 \mathrm{d}t}{\sum_{n=1}^N \int_0^m \left(\mathbf{W_{u\cdot v,n}}(t)\right)^2 \mathrm{d}t} \qquad =: \mathcal{H}_2^{m,+}(s) \qquad (16)$$

and

$$\hat{H}_3^{m,+}(s) \Rightarrow \frac{\sum_{n=1}^N \left(\int_m^s \mathbf{W_{u\cdot v,n}}(t)\mathrm{d}t\right)^2}{\sum_{n=1}^N \left(\int_0^m \mathbf{W_{u\cdot v,n}}(t)\mathrm{d}t\right)^2} \qquad =: \mathcal{H}_3^{m,+}(s), \qquad (17)$$

for $T \to \infty$, where the specific form of $\mathbf{W_{u\cdot v,n}}(s)$ depends on which of the three situations is considered. (15) - (17) are only valid provided the denominators of (11) - (13) and their respective limits are invertible.

We reject the null hypothesis if the weighted detector $\frac{\hat{H}^{m,+}(s)}{g(s)}$ exceeds a critical value for the first time where $\hat{H}^{m,+}(s)$ is any of the above detectors. This point in time is referred to as detection time, i.e.

$$\tau_m := \min_{s:[mT]+1 \leq [sT] \leq T} \left\{ \frac{\hat{H}^{m,+}(s)}{g(s)} > c \right\}, \qquad (18)$$

where $g(s)$ is a weighting function that has to be chosen. If $\frac{\hat{H}^{m,+}(s)}{g(s)} \leq c$ for all $m \leq s \leq 1$, set $\tau_m := \infty$. Hence, a finite value of τ_m implies a rejection of the null hypothesis and serves as an immediate estimate of the potential breakpoint. The critical value c and the weighting function $g(s)$ have to be chosen such that under the null hypothesis it holds that

$$\begin{aligned}
\lim_{T\to\infty} \mathbb{P}\left(\tau_m < \infty\right) &= \lim_{T\to\infty} \mathbb{P}\left(\min_{s:[mT]+1\leq[sT]\leq T}\left\{\frac{\hat{H}^{m,+}(s)}{g(s)} > c\right\} < \infty\right) \\
&= \lim_{T\to\infty} \mathbb{P}\left(\sup_{s:[mT]+1\leq[sT]\leq T}\frac{\hat{H}^{m,+}(s)}{g(s)} > c\right) \qquad (19) \\
&= \mathbb{P}\left(\sup_{m\leq s\leq 1}\frac{\mathcal{H}^{m,+}(s)}{g(s)} > c\right) = \alpha,
\end{aligned}$$

where α denotes the chosen significance level. We only allow continuous, positive and bounded weighting functions. Clearly, τ_m and c depend on the chosen detector as well as on m, the deterministic trend D_t and the number of regressors k. According to (19), the decision rule to reject the null hypothesis if $\tau_m < \infty$ is equivalent to rejecting the null hypothesis if $\sup_{s:[mT]+1\leq[sT]\leq T}\frac{\hat{H}^{m,+}(s)}{g(s)} > c$.

Using the established limits and the continuous mapping theorem we derive:

Theorem 1. *Let the assumptions of Lemma 1 be in place and assume that $g(s)$ is*

Detector	$D_t = 1$	$D_t = [1, t]'$
$\mathbb{E}(\mathcal{H}_1^{m,+}(s))$	s^2	s^4
$\mathbb{E}(\mathcal{H}_2^{m,+}(s))$	s^3	s^5
$\mathbb{E}(\mathcal{H}_3^{m,+}(s))$	s^4	s^6

Table 1: Order of the expected values of the limiting distributions (15) - (17) in the case of intercept only ($D_t = 1$) or linear trend ($D_t = [1, t]'$) and no regressors, $\dim X_t = 0$.

continuous with $0 < g(s) < \infty$ for $m \le s \le 1$. Then, under the null hypothesis there exist for any $0 < \alpha < 1$ critical values $c = c(\alpha, g, \hat{H}_i^{m,+})$, such that

$$\lim_{T \to \infty} \mathbb{P}\left(\tau_m(g, c(\alpha, g, \hat{H}_i^{m,+})) < \infty\right) = \alpha, \tag{20}$$

for $i = 1, \dots, 3$.

We calculate the order of the expected value of the three limit processes to motivate our choice of $g(s)$ for intercept and linear trend since optimal weighting functions, e.g. in the sense of minimum detection delay, are in general not deducible (see Chu et al., 1996). Hence, we use the monoms matching the respective detector displayed in Table 1 for the cases intercept only or linear trend, and arbitrary number of regressors k. In order to calculate the critical value $c(\alpha, g, \hat{H}_i^{m,+})$ we need to simulate the limiting distribution $\frac{\mathcal{H}_i^{m,+}(s)}{g(s)}$ by approximating the functionals of Brownian motions by the corresponding functions of random walks.

Finally, we introduce some additional notation. With the stacked errors $\eta_{n,t} := [u_{n,t}, v'_{n,t}]'$ associated to individual cointegrating regressions we define long-run and one-sided long-run covariances of $\eta_{n,t}$ as

$$\Omega^{m,n} = \begin{pmatrix} \Omega_{uu}^{m,n} & \Omega_{uv}^{m,n} \\ \Omega_{vu}^{m,n} & \Omega_{vv}^{m,n} \end{pmatrix} := \sum_{h=-\infty}^{\infty} \mathbb{E}(\eta_{m,0}\eta'_{n,h}),$$

$$\Delta^{m,n} = \begin{pmatrix} \Delta_{uu}^{m,n} & \Delta_{uv}^{m,n} \\ \Delta_{vu}^{m,n} & \Delta_{vv}^{m,n} \end{pmatrix} := \sum_{h=0}^{\infty} \mathbb{E}(\eta_{m,0}\eta'_{n,h}),$$

$$\Omega_{ij}^{m,\cdot} := [\Omega_{ij}^{m,1}, \dots, \Omega_{ij}^{m,N}]$$

and

$$\Delta_{ij}^{m,\cdot} := [\Delta_{ij}^{m,1}, \dots, \Delta_{ij}^{m,N}]$$

for $i, j = u$ and v and $m, n = 1, \ldots, N$. In what follows we denote consistent estimators of the (one-sided) long-run variance based on the calibration period with a subscript m and "$\wedge$" on top. By $(A)_{n,\cdot}$ we denote the n-th row of a matrix A. $\mathbf{I}_n$ is an $n \times n$ unity matrix and $\mathbf{1}_{n \times m}$ is an $n \times m$ matrix of ones.

2.1. Uncorrelated Homogeneous Cointegrating Regressions

We consider homogeneous cointegrating relationships by imposing the following additional assumption of cross-sectionally identical parameters:

Assumption 3. $\theta_D = \theta_{D,n}$ and $\theta_X = \theta_{X,n}$ for all $n = 1, \ldots, N$.

Assumption 3 implies

$$y_{n,t} = \begin{cases} D'_t \theta_D + X'_{n,t} \theta_X + u_{n,t}, & t = 1, \ldots, [rT], \\ D'_t \theta_{D,1,n} + X'_{n,t} \theta_{X,1,n} + u_{n,t}, & t = [rT] + 1, \ldots, T, \end{cases} \tag{21}$$

and

$$\Delta X_{n,t} = v_{n,t}, \quad t = 1, \ldots, T, \tag{22}$$

for $n = 1, \ldots, N$, and simplifies the null hypothesis and alternative with regards to the parameters θ_D and θ_X. Under the null hypothesis no structural change occurs, i.e. $\theta := [\theta'_D, \theta'_X]' = [\theta'_{D,1,n}, \theta'_{X,1,n}]' =: \theta_{1,n}$ and under the alternative there is a change in at least one cointegrating regression. Consequently,

$$H_0 : \begin{cases} \theta = \theta_{1,n} \text{ for all } m \leq r < 1, n = 1, \ldots, N, \text{ and} \\ \{u_{n,t}\}_{t=1,\ldots,T} \text{ is I(0) for all } n = 1, \ldots, N \end{cases} \tag{23}$$

and

$$H_1 : \begin{cases} \theta \neq \theta_{1,n} \text{ for some } m \leq r < 1, n \in \{1, \ldots, N\} \textbf{ or} \\ \{u_{n,t}\}_{t=1,\ldots,[rT]} \text{ is I(0) and } \{u_{n,t}\}_{t=[rT]+1,\ldots,T} \text{ is I(1)} \\ \text{for some } m \leq r < 1, n \in \{1, \ldots, N\} \end{cases} \tag{24}$$

Note that under the alternative of a parameter change the system may turn heterogeneous, i.e. $\theta_{1,i} \neq \theta_{1,j}$ for some $i, j \in \{1, \ldots, N\}$, or stay homogeneous with $\theta_{1,i} = \theta_{1,j}$ for all $i, j \in \{1, \ldots, N\}$.

With regards to the errors we assume a naive i.i.d. setting at first, namely:

Assumption 4. *The stacked error processes $\{\eta_{n,t} := [u_{n,t}, v'_{n,t}]'\}_{t=1,\ldots,T}$ are independent and identically distributed for all n.*

Note that by Assumption 4

$$\Omega^{n,n} = \Omega^{\nu,\nu},$$
$$\Delta^{n,n} = \Delta^{\nu,\nu}$$

for all $n, \nu = 1, \ldots, N$ and

$$\Omega^{n,\nu} = \Delta^{n,\nu} = 0$$

for all $n, \nu = 1, \ldots, N, n \neq \nu$. Due to the above implication the decomposition of $B(s)$ collapses to

$$B(s) = \Omega^{1/2} W(s) = \begin{bmatrix} \mathbf{I_N} \otimes \Omega_{uu}^{1,1} & \mathbf{I_N} \otimes \Omega_{vu}^{1,1} \\ \mathbf{I_N} \otimes \Omega_{uv}^{1,1} & \mathbf{I_N} \otimes \Omega_{vv}^{1,1} \end{bmatrix}^{1/2} W(s),$$

a simpler linear transformation of standard Brownian motions where

$$\Omega^{1/2} := \begin{bmatrix} \mathbf{I_N} \otimes \omega_{u\cdot v} & \mathbf{I_N} \otimes \lambda_{uv} \\ \mathbf{I_N} \otimes \mathbf{0_{k\times 1}} & \mathbf{I_N} \otimes \Omega_{vv}^{1/2} \end{bmatrix} \text{ and } \left(\Omega^{1,1}\right)^{1/2} := \begin{bmatrix} \omega_{u\cdot v} & \lambda_{uv} \\ \mathbf{0_{k\times 1}} & (\Omega_{vv}^{1,1})^{1/2} \end{bmatrix} \quad (25)$$

with $\omega_{u\cdot v}^2 := \Omega_{uu}^{1,1} - \Omega_{uv}^{1,1}(\Omega_{vv}^{1,1})^{-1}\Omega_{vu}^{1,1}$ and $\lambda_{uv} := \Omega_{uv}^{1,1}(\Omega_{vv}^{1,1})^{-1/2}$. Then $\Omega^{1/2}\left(\Omega^{1/2}\right)' = \Omega$ and

$$\begin{bmatrix} \mathbf{I_N} \otimes \omega_{u\cdot v} & \mathbf{I_N} \otimes \lambda_{uv} \\ \mathbf{I_N} \otimes \mathbf{0_{k\times 1}} & \mathbf{I_N} \otimes (\Omega_{vv}^{1,1})^{1/2} \end{bmatrix} \begin{bmatrix} \mathbf{I_N} \otimes \omega_{u\cdot v} & \mathbf{I_N} \otimes \lambda_{uv} \\ \mathbf{I_N} \otimes \mathbf{0_{k\times 1}} & \mathbf{I_N} \otimes (\Omega_{vv}^{1,1})^{1/2} \end{bmatrix}' = \begin{bmatrix} \mathbf{I_N} \otimes \Omega_{uu}^{1,1} & \mathbf{I_N} \otimes \Omega_{vu}^{1,1} \\ \mathbf{I_N} \otimes \Omega_{uv}^{1,1} & \mathbf{I_N} \otimes \Omega_{vv}^{1,1} \end{bmatrix}$$

hold, respectively. Here, the assumption $\Omega_{vv}^{1,1} > 0$ suffices to exclude cointegration among the regressors $X_{n,t}$ for fixed n which is typically assumed for FM-OLS estimation. Then, Assumption 4 implies no cointegration across X_t.

In order to obtain nuisance parameter free asymptotic distributions of the monitoring statistics we use the PFM-OLS estimator of Phillips and Moon (1999, Section 5.2) for systems of homogeneous cointegrating regressions.

Define $Z_{n,t} := [D_t', X_{n,t}']'$ and $Z_t := [Z_{1,t}, \ldots, Z_{N,t}]$ and we have

$$
y_t = \begin{bmatrix} y_{1,t} \\ \vdots \\ y_{N,t} \end{bmatrix} = \begin{bmatrix} D_t' & X_{1,t}' \\ \vdots & \vdots \\ D_t' & X_{N,t}' \end{bmatrix} \begin{bmatrix} \theta_D \\ \theta_X \end{bmatrix} + \begin{bmatrix} u_{1,t} \\ \vdots \\ u_{N,t} \end{bmatrix} = Z_t'\theta + u_t
$$

due to Assumption 3. Since we assume cross-sectional homogeneity and independence, we can modify the dependent variables by using

$$
y_{n,t;m}^+ := y_{n,t} - \hat{\Omega}_{uv;m}^{1,1}(\hat{\Omega}_{vv;m}^{1,1})^{-1}\Delta X_{n,t} \tag{26}
$$

and

$$
\hat{\Delta}_{vu;m}^+ := \hat{\Delta}_{vu;m}^{1,1} - \hat{\Delta}_{vv;m}^{1,1}(\hat{\Omega}_{vv;m}^{1,1})^{-1}\hat{\Omega}_{vu;m}^{1,1}, \tag{27}
$$

where all estimators indicate the arithmetic mean of the respective non-parametric kernel estimators based on the cointegrating regressions and the pre-break sample $1, \ldots, [mT]$, e.g. $\hat{\Omega}_{vv;m}^{1,1} = N^{-1}\sum_{n=1}^N \hat{\Omega}_{vv,n;m}^{1,1}$, where $\hat{\Omega}_{vv,n;m}^{1,1}$ is based solely on cointegrating regression n. Long-run variances are estimated using the stacked error processes $\hat{\eta}_{n,t} := [\hat{u}_{n,t;m}, v_{n,t}']'$ for $t = 2, \ldots, [mT]$ with $\hat{u}_{n,t;m}$ the OLS residuals resulting from individual estimation using the calibration period. We assume that long-run variances are estimated consistently, e. g. under the assumptions of Jansson (2002). The PFM-OLS estimator is given by

$$
\begin{aligned}
\hat{\theta}_{m,\text{PFM}} &:= \left(\sum_{t=1}^{[mT]} \sum_{n=1}^N Z_{n,t}Z_{n,t}' \right)^{-1} \left(\sum_{t=1}^{[mT]} \sum_{n=1}^N Z_{n,t}y_{n,t;m}^+ - N[mT]\begin{bmatrix} \mathbf{0_{p\times 1}} \\ \hat{\Delta}_{vu;m}^+ \end{bmatrix} \right) \\
&= \left(\sum_{t=1}^{[mT]} Z_t Z_t' \right)^{-1} \left(\sum_{t=1}^{[mT]} Z_t y_{t;m}^+ - N[mT]\begin{bmatrix} \mathbf{0_{p\times 1}} \\ \hat{\Delta}_{vu;m}^+ \end{bmatrix} \right),
\end{aligned} \tag{28}
$$

where $y_{t;m}^+ = [y_{1,t;m}^+, \ldots, y_{N,t;m}^+]'$.

Note, that Phillips and Moon (1999) consider a panel structure with simultaneously $\{T, N\} \to \infty$, while we confine ourselves to the case $T \to \infty$ and N fixed. Another methodological difference is that they work with random linear error processes (VMA(∞)-processes with random coefficients) and show in their Lemma 3 that they fulfill a panel functional central limit theorem under certain assumptions on the random coefficients (Assumption 1 and 2 in their paper, mainly an i.i.d. assumption and moment conditions; for homogeneous panel cointegration they strengthen these to non-random coefficients). That means Phillips and Moon (1999) work with "low-level" assumptions on the error structure while we employ the "high-level" Assumption 2 that the errors follow a functional

central limit theorem, which in fact is a result based on structural assumptions on the errors. Any set of assumptions that implies Assumption 2 is suitable for our purpose.

We derive (c.f. Phillips and Hansen, 1990) the following result concerning the asymptotic behaviour of the PFM-OLS estimator:

Lemma 2. *Let the data be generated by (21) and (22) with Assumptions 1 - 4 in place. Then*

$$G_T^{-1}\left(\hat{\theta}_{m,PFM} - \theta\right) \Rightarrow \omega_{u\cdot v}\left(\sum_{n=1}^{N}\int_0^m J_n(r)J_n(r)'\mathrm{d}r\right)^{-1} \tag{29}$$
$$\times \left(\sum_{n=1}^{N}\int_0^m J_n(r)\mathrm{d}W_{u\cdot v,n}(r)\right),$$

as $T \to \infty$ with $J_n(r) := [D(r)', B_{v,n}(r)']'$, $G_T := \mathrm{diag}(G_{D,T}, G_{X,T})$ and $G_{X,T} := T^{-1}\mathbf{I_k}$.

The corresponding N-dimensional residuals are given by $\hat{u}_{t;m,PFM}^+ := y_{t;m}^+ - Z_t'\hat{\theta}_{m,PFM} = u_t - V_t'(\hat{\Omega}_{vv;m}^{1,1})^{-1}\hat{\Omega}_{vu;m}^{1,1} - Z_t'(\hat{\theta}_{m,PFM} - \theta)$ with $V_t := [v_{1,t}, \ldots, v_{N,t}]$ and we obtain the following limiting distribution for the scaled partial sum process:

Lemma 3. *Let the data be generated by (21) and (22) with Assumptions 1 - 4 in place. Then it holds under the null hypothesis and for $0 \leq s \leq 1$*

$$T^{-1/2}\sum_{t=1}^{[sT]}\hat{u}_{t;m,PFM}^+ \Rightarrow \omega_{u\cdot v}\left\{W_{u\cdot v}(s) - \int_0^s J(r)'\mathrm{d}r\left(\sum_{n=1}^{N}\int_0^m J_n(r)J_n(r)'\mathrm{d}r\right)^{-1}\right. \tag{30}$$
$$\left.\times\left(\sum_{n=1}^{N}\int_0^m J_n(r)\mathrm{d}W_{u\cdot v,n}(r)\right)\right\} =: \omega_{u\cdot v}\widehat{W}_{u\cdot v}(s)$$

for $T \to \infty$ with $J(r) := [J_1(r), \ldots, J_N(r)]$ and $J_n(r) = [D(r)', W_{v,n}(r)']'$.

Note that the process $\widehat{W}_{u\cdot v}(s)$ depends on m, the deterministic trend D_t and the number of regressors k as well but we do not reflect this in our notation.

Under Assumptions 3 and 4 self-normalization cancels out the long-run variance in the detector limit. Hence, we get rid of the well-known and unwanted finite sample size distortions induced by long-run variance estimation. A crucial ingredient here is the homogeneity of long-run variances. Assume for this paragraph that $\omega_{u\cdot v,n}^2$ is the conditional long-run variance in cointegrating relation n and that the conditional long-run

variances are not homogeneous across cointegrating relations, i.e. $\omega_{u\cdot v,1}^2 \neq \omega_{u\cdot v,n}^2$ for some $n \in \{2,\ldots,N\}$. Then, (29) changes to

$$G_T^{-1}(\hat{\theta}_{m,\text{PFM}} - \theta) \Rightarrow \left(\sum_{n=1}^N \int_0^m J_n(r)J_n(r)'\mathrm{d}r\right)^{-1} \left(\sum_{n=1}^N \omega_{u\cdot v,n} \int_0^m J_n(r)\mathrm{d}W_{u\cdot v,n}(r)\right)$$

for $T \to \infty$, and the j-th component of (30), $T^{-1/2}\sum_{t=1}^{[sT]} \hat{u}_{j,t;m,\text{PFM}}^+$, converges weakly to

$$\omega_{u\cdot v,j} W_{u\cdot v,j}(s)$$
$$- \int_0^s J_j(r)'\mathrm{d}r \left(\sum_{n=1}^N \int_0^m J_n(r)J_n(r)'\mathrm{d}r\right)^{-1} \left(\sum_{n=1}^N \omega_{u\cdot v,n} \int_0^m J_n(r)\mathrm{d}W_{u\cdot v,n}(r)\right)$$

for $T \to \infty$, where the convergence still holds jointly for all $j = 1,\ldots,N$. The nuisance parameters $\omega_{u\cdot v,n}$ cannot be scaled out in the detectors due to their heterogeneity.

Homogeneous parameters are a crucial assumption for (30) as in case of heterogeneous parameters (29) is no longer valid and $\hat{\theta}_{m,\text{PFM}}$ is only consistent for the average parameter across all equations (c.f. Phillips and Moon, 1999, p. 1080, remark (c), and recall we do not consider random, but fixed parameters).

The limiting distributions depend on different parameters and we obtain critical values for a selection of them, namely $D_t = 1$ or $D_t = [1,t]'$, using the weighting function corresponding to D_t and the respective detector (c.f. Table 1), m-values ranging from 0.1 to 0.9 with mesh 0.01, $N = 1, 2, 3, 5, 10, 20, 30$ and $k = 1,\ldots,4$. We provide further details on simulating the critical values in the additional material.

2.2. Correlated Homogeneous Cointegrating Regressions

As in Section 2.1, the data are generated by (21) and (22) as we consider monitoring homogeneous cointegrating relationships. Regarding the errors we abandon Assumption 4 of independent and identically distributed error vectors η_t but allow for arbitrary dependence among the regressors – except cointegration among the regressors, i.e. $\Omega_{vv}^{n,n} > 0$ and $\Omega_{vv} > 0$ hold. In this case, the modified dependent variable is $y_{t;m,\text{GLS}}^+ :=$ $y_t - \hat{\Omega}_{uv;m}\hat{\Omega}_{vv;m}^{-1}\Delta X_t$ and due to cross-sectional dependence we use the bias correction

term

$$\hat{\delta}_m := \sum_{n=1}^{N} \begin{bmatrix} \mathbf{0_{p \times 1}} \\ (\hat{\Delta}_{vu;m}^{n,\cdot})((\hat{\Omega}_{u \cdot v;m}^{-1})_{n,\cdot})' - \hat{\Delta}_{vv;m}^{n,\cdot}((\hat{\Omega}_{u \cdot v;m}^{-1}\hat{\Omega}_{uv;m}\hat{\Omega}_{vv;m}^{-1})_{n,\cdot})' \end{bmatrix}. \tag{31}$$

$\hat{\Omega}_{u \cdot v;m}$ is an estimator of $\Omega_{u \cdot v} := \Omega_{uu} - \Omega_{uv}\Omega_{vv}^{-1}\Omega_{vu}$, the long-run covariance of the modified system error $u_{t;m,\text{GLS}}^{+} := u_t - \hat{\Omega}_{uv;m}\hat{\Omega}_{vv;m}^{-1}\Delta X_t$. In order to deal with an arbitrary error structure, we use the pooled feasible GLS estimator

$$\hat{\theta}_{m,\text{PFM-GLS}} := \left(\sum_{t=1}^{[mT]} Z_t \hat{\Omega}_{u \cdot v;m}^{-1} Z_t' \right)^{-1} \left(\sum_{t=1}^{[mT]} Z_t \hat{\Omega}_{u \cdot v;m}^{-1} y_{t;m,\text{GLS}}^{+} - [mT]\hat{\delta}_m \right) \tag{32}$$

of the modified system.

Lemma 4. *Let the data be generated by (21) and (22) with Assumptions 1 - 3 in place. Then*

$$G_T^{-1}(\hat{\theta}_{m,PFM\text{-}GLS} - \theta) \Rightarrow \left(\int_0^m J(r)\Omega_{u \cdot v;m}^{-1} J(r)' \mathrm{d}r \right)^{-1} \left(\int_0^m J(r)\Omega_{u \cdot v;m}^{-1/2} \mathrm{d}W_{u \cdot v}(r) \right) \tag{33}$$

as $T \to \infty$ with $J_n(r) = [D(r)', B(r)_{v,n}']'$, $J(r) := [J_1(r), \ldots, J_N(r)]$, $G_T = \mathrm{diag}(G_{D,T}, G_{X,T})$ and $G_{X,T} = T^{-1}\mathbf{I_k}$.

Here, the residual vector is $\hat{u}_{t;m,\text{PFM-GLS}}^{+} := y_{t;m,\text{GLS}}^{+} - Z_t'\hat{\theta}_{\text{PFM-GLS}} = u_t - \hat{\Omega}_{uv;m}\hat{\Omega}_{vv;m}^{-1}v_t - Z_t'(\hat{\theta}_{\text{PFM-FGLS}} - \theta)$ and the following Lemma holds for the scaled partial sum process:

Lemma 5. *Let the data be generated by (21) and (22) with Assumptions 1 - 3 in place. Then it holds under the null hypothesis and for $0 \le s \le 1$*

$$T^{-1/2}\sum_{t=1}^{[sT]} \hat{u}_{t;m,PFM\text{-}GLS}^{+} \Rightarrow \Omega_{u \cdot v;m}^{1/2}W_{u \cdot v}(s) - \int_0^s J(r)' \mathrm{d}r \left(\int_0^m J(r)\Omega_{u \cdot v;m}^{-1} J(r)' \mathrm{d}r \right)^{-1}$$
$$\times \left(\int_0^m J(r)\Omega_{u \cdot v;m}^{-1/2} \mathrm{d}W_{u \cdot v}(r) \right) \tag{34}$$

as $T \to \infty$ with $J_n(r) = [D(r)', B(r)_{v,n}']'$ and $J(r) = [J_1(r), \ldots, J_N(r)]$.

The limiting distribution does not only depend on the deterministic trend D_t, the weighting function g and the parameters m, N and k but on the long-run covariance structure as well. This renders tabulating simulated critical values infeasible. In order to perform hypotheses tests we need to estimate Ω consistently and replace nuisance

parameters in the limiting distribution by consistent estimators. Then, we simulate critical values under the null hypothesis based on independent copies of $W(s)$ that we can easily transform into $B(s)$ to calculate independent copies of $J(s)$ by plugging in covariance estimates performed on the calibration period.

2.3. Seemingly Unrelated Cointegrating Regressions

Suppose now that the cointegrating regressions have individual parameters and the error vectors are not cross-sectionally independent, i.e. we abandon Assumptions 3 and 4 and the data are generated by (1) and (2). By defining $\mathbf{Z}_t := \text{diag}(Z_{1,t}, \ldots, Z_{N,t})$ and $\theta := [\theta_1', \ldots, \theta_N']'$ we have

$$y_t = \mathbf{Z}_t'\theta + u_t. \tag{35}$$

For fully modified estimation we use the GLS modified dependent variable $y_{t;m,\text{GLS}}^+$ and the bias correction term $\hat{\phi}_m := [\hat{\phi}_{1;m}', \ldots, \hat{\phi}_{N;m}']'$ with $\hat{\phi}_{n;m} := [\mathbf{0}_{\mathbf{p}\times\mathbf{1}}', ((\Delta_{vu;m}^{n,\cdot})^+)']'$ and

$$(\Delta_{vu;m}^{n,\cdot})^+ := (\hat{\Delta}_{vu;m}^{n,\cdot})((\hat{\Omega}_{u\cdot v;m}^{-1})_{n,\cdot})' - \hat{\Delta}_{vv;m}^{n,\cdot}((\hat{\Omega}_{u\cdot v;m}^{-1}\hat{\Omega}_{uv;m}\hat{\Omega}_{vv;m}^{-1})_{n,\cdot})'. \tag{36}$$

Moon (1999) discusses three different estimators for this model where the fully modified SUR estimator

$$\hat{\theta}_{\text{FM-SUR}} := \left(\sum_{t=1}^{[mT]} \mathbf{Z}_t\hat{\Omega}_{u\cdot v;m}^{-1}\mathbf{Z}_t'\right)^{-1} \left(\sum_{t=1}^{[mT]} \mathbf{Z}_t\hat{\Omega}_{u\cdot v;m}^{-1}y_{t;m,\text{GLS}}^+ - [mT]\hat{\phi}_m\right), \tag{37}$$

is the feasible GLS estimator and efficient among those three estimators (c.f. Park and Ogaki, 1991, for additional details on the efficiency).

Lemma 6. *Let the data be generated by (1) and (2) with Assumptions 1 and 2 in place. Then*

$$\mathbf{G}_T^{-1}(\hat{\theta}_{FM\text{-}SUR} - \theta) \Rightarrow \left(\int_0^m \mathbf{J}(r)\Omega_{u\cdot v;m}^{-1}\mathbf{J}(r)'\mathrm{d}r\right)^{-1} \left(\int_0^m \mathbf{J}(r)\Omega_{u\cdot v;m}^{-1/2}\mathrm{d}W_{u\cdot v}(r)\right) \tag{38}$$

as $T \to \infty$ with $J_n(r) = [D(r)', B_{v,n}(r)']'$, $\mathbf{J}(r) := \text{diag}(J_1(r), \ldots J_N(r))$ and $\mathbf{G}_T := \mathbf{I}_N \otimes \text{diag}(G_{D,T}, G_{X,T})$, $G_{X,T} = T^{-1}\mathbf{I_k}$.

Here, the residual vectors are given by $\hat{u}_{t;m,\text{FM-SUR}}^{+} := y_{t;m,\text{GLS}}^{+} - \mathbf{Z}_t'\hat{\theta}_{\text{FM-SUR}} = u_t - \hat{\Omega}_{uv;m}\hat{\Omega}_{vv;m}^{-1}v_t - \mathbf{Z}_t'(\hat{\theta}_{\text{FM-SUR}} - \theta)$ and the scaled partial sum process of the modified residuals has the following probability limit:

Lemma 7. *Let the data be generated by (1) and (2) with Assumptions 1 and 2 in place. Then it holds under the null hypothesis and for $0 \leq s \leq 1$*

$$T^{-1/2}\sum_{t=1}^{[sT]}\hat{u}_{t;m,FM\text{-}SUR}^{+} \Rightarrow \Omega_{u\cdot v;m}^{1/2}W_{u\cdot v}(s) - \int_0^s \mathbf{J}(r)'\mathrm{d}r\left(\int_0^m \mathbf{J}(r)\Omega_{u\cdot v;m}^{-1}\mathbf{J}(r)'\mathrm{d}r\right)^{-1} \times \left(\int_0^m \mathbf{J}(r)\Omega_{u\cdot v;m}^{-1/2}\mathrm{d}W_{u\cdot v}(r)\right) \tag{39}$$

as $T \to \infty$ with $J_n(r) = [D(r)', B(r)'_{v,n}]'$ and $\mathbf{J}(r) = \mathrm{diag}(J_1(r),\ldots J_N(r))$.

Note that, $\sum_{i=1}^{[mT]}\sum_{t=1}^{i}\hat{u}_{t,\text{FM-SUR}}^{+} = 0$ if the regression contains an intercept and a linear trend, and $\sum_{t=1}^{[mT]}\hat{u}_{t,\text{FM-SUR}}^{+} = 0$ if the regression contains an intercept. Thus, (15) and (17) are not valid in the respective cases.

As in Lemma 5, the limiting distribution depends on the long-run covariance structure and renders tabulating simulatd critical values infeasible. Again, we estimate Ω consistently, replace nuisance parameters in the limiting distribution by consistent estimators and simulate critical values under the null hypothesis based on independent copies of $W(s)$ and covariance estimates from the calibration period.

3. Finite Sample Performance

We investigate the finite sample properties of the monitoring procedures based on the different detectors and estimators by means of a simulation study. First, we consider the detectors from Section 2.1 for cross-sectional independence and homogenous parameters, then we move to the detectors from Section 2.2 and 2.3. We extend the data generating process used by Vogelsang and Wagner (2014) and Wagner and Wied (2017):

$$y_{n,t} = \mu + \gamma t + x_{n,t,1}\beta_1 + x_{n,t,2}\beta_2 + u_{n,t},$$
$$x_{n,t,i} = x_{n,t-1,i} + v_{n,t,i}, \quad x_{n,0,i} = 0, \quad i = 1, 2, \tag{40}$$

where

$$u_{n,t} = \rho_1 u_{n,t-1} + \varepsilon_{n,t} + \rho_2(e_{n,t,1} + e_{n,t,2}), \quad u_{n,0} = 0,$$
$$v_{n,t,i} = e_{n,t,i} + 0.5 e_{n,t-1,i}, \quad i = 1, 2, \tag{41}$$

for $t = 1, \ldots, [mT]$. $\varepsilon_{n,t}$, $e_{n,t,1}$ and $e_{n,t,2}$ are i.i.d. standard normal random variables independent of each other. The chosen parameter values are $\mu = 3, \beta_1, \beta_2, \gamma = 1$. The values for ρ_1 and ρ_2 are chosen from the set $\{0.3, 0.6\}$. The parameter ρ_2 controls the serial correlation in the regression error and is set to $\rho_1 = 1$ under the alternative of I(1) errors, whereas the parameter ρ_2 controls whether the regressors are endogenous ($\rho_2 \neq 0$) or not ($\rho_2 = 0$).

By this simulation study we investigate which of the detectors $\hat{H}_1^{m,+}$, $\hat{H}_2^{m,+}$ and $\hat{H}_3^{m,+}$ is best in the sense of finite sample size control under the null hypothesis as well as power and detection delay under different alternatives. We are interested in how heterogeneous parameters affect the detectors and investigate what happens if we consider alternatives with different regression parameters cross-sectionally by using alternative parameter estimators discussed in Sections 2.2 and 2.3. An additional important question is how the detectors perform if structural breaks occur only in a fraction of the cointegrating regressions.

We consider different versions (or in some cases modifications) of (40) and (41) for $t = [mT] + 1, \ldots, T$ to answer the posed questions. In some scenarios we vary the model in the calibration period $t = 1, \ldots, [mT]$ as well. All hypothesis tests are performed on a 5% significance level and we consider combinations of $m \in \{0.10, 0.11, \ldots, 0.89, 0.90\}$ and $N \in \{1, 2, 3, 5, 10, 20, 30\}$.

3.1. Null Rejection Probability in Uncorrelated Homogeneous Cointegrating Regressions

In this section, we analyze the behavior of the detectors from Section 2.1 based on PFM-OLS estimation. We additionally assume (40) and (41) for $t = [mT] + 1, \ldots, T$ to investigate the finite sample performance under the null hypothesis. In particular we are interested whether the null rejection probability is reasonably close to the nominal significance level of 5%.

In general the null rejection probability is close to the significance level. The detectors suffer from larger long-run variances induced by higher regressor endogeneity and higher
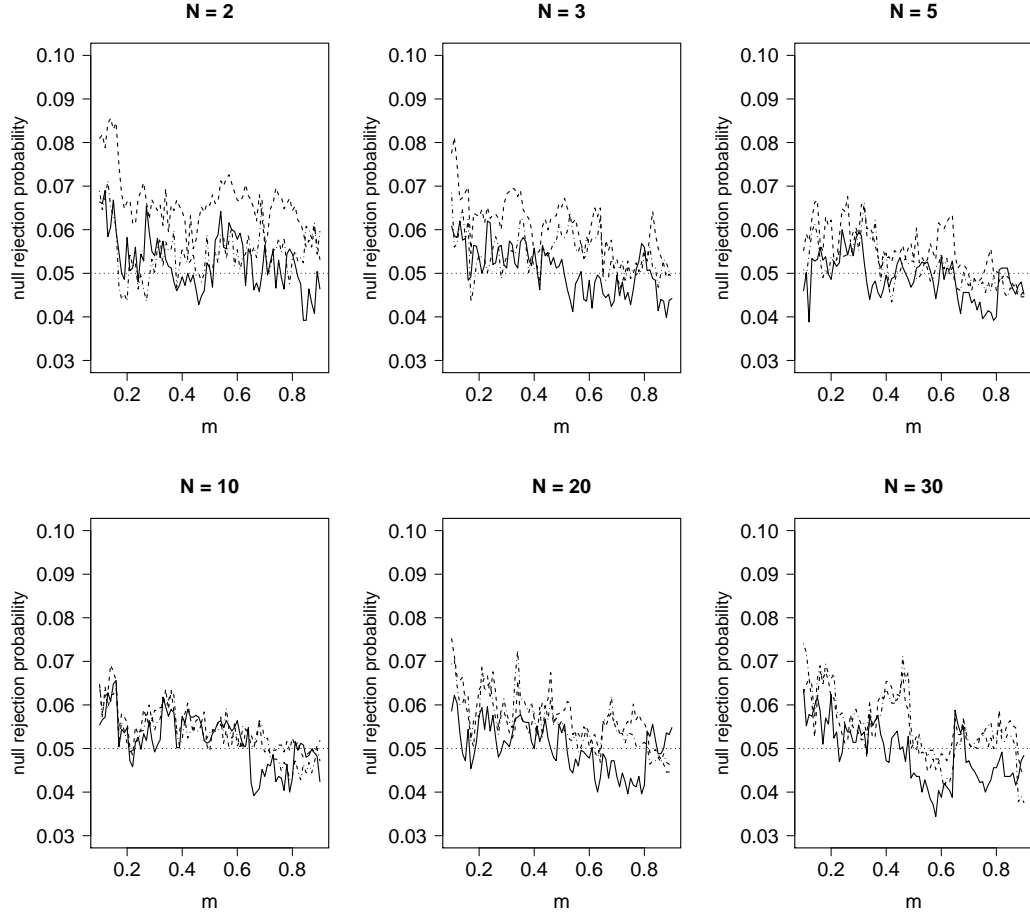
Figure 2: Null rejection probability in uncorrelated homogeneous cointegrating regressions (Section 3.1) with $T = 500$, $\rho_1 = \rho_2 = 0.3$ and PFM-OLS estimation. The lines represent $\hat{H}_{1,\text{PFM}}^{m,+}$ (solid), $\hat{H}_{2,\text{PFM}}^{m,+}$ (dashed) and $\hat{H}_{3,\text{PFM}}^{m,+}$ (dotdashed).
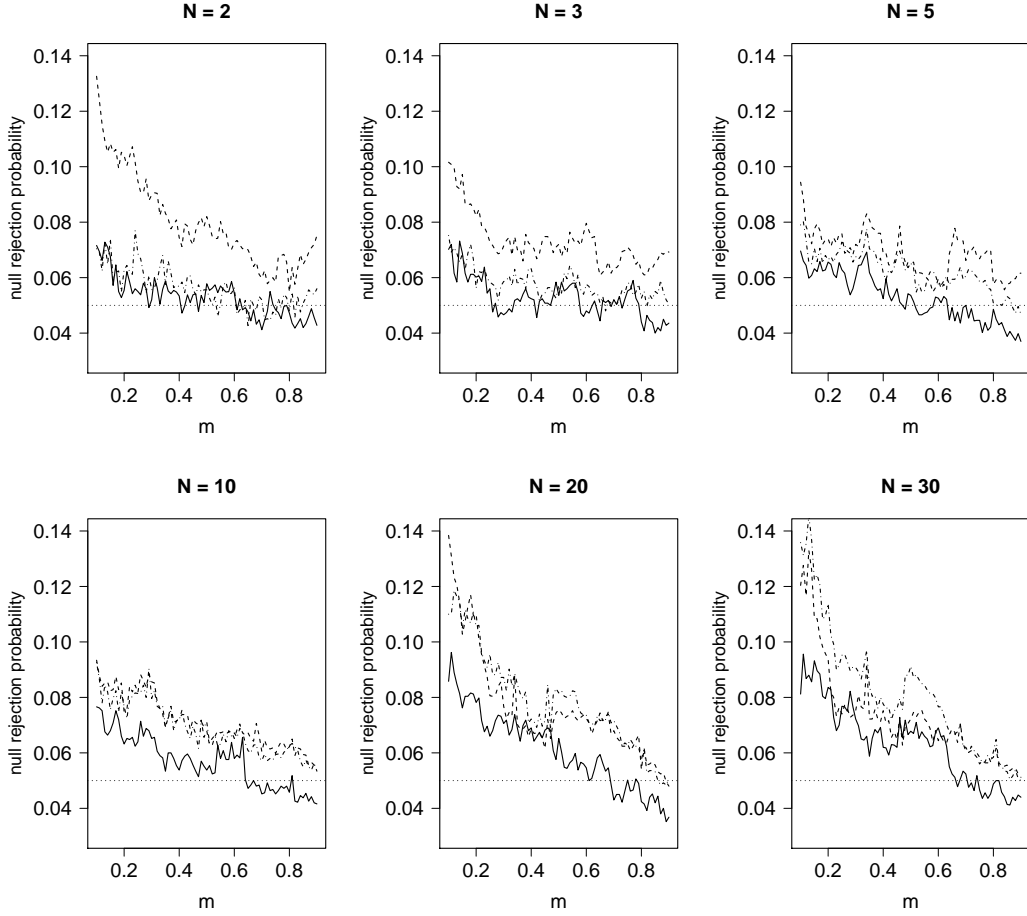
Figure 3: Null rejection probability in uncorrelated homogeneous cointegrating regressions (Section 3.1) with $T = 500$, $\rho_1 = \rho_2 = 0.6$ and PFM-OLS estimation. The lines represent $\hat{H}_{1,\text{PFM}}^{m,+}$ (solid), $\hat{H}_{2,\text{PFM}}^{m,+}$ (dashed) and $\hat{H}_{3,\text{PFM}}^{m,+}$ (dotdashed).

error serial correlation. For $N = 2, 3, 5$ the detectors work reasonably well and the null rejection probability decreases in m, size distortions come up for $N = 10$ and get even larger for $N = 20, 30$. All size distortions we observe decrease in m as we use $[mT]$ observations for estimation in the calibration period. $\hat{H}_{1,\text{PFM}}^{m,+}$ seems to perform best in the sense of null rejection probability in this case. Note that $\hat{H}_{1,\text{PFM}}^{m,+}$ and $\hat{H}_{3,\text{PFM}}^{m,+}$ do not work for $N = 1$ due to the presence of an intercept and a linear trend in D_t (see Lemma 1 and the remark after Lemma 7 which holds for PFM-OLS and $N = 1$ as well).

In Figure 2 the case $T = 500$ and $\rho_1 = \rho_2 = 0.3$ is shown. The detectors behave similarly well and the null rejection probabilities are close to the significance level ranging between

0.04 and 0.07. In the case of $T = 500$ and $\rho_1 = \rho_2 = 0.6$ (Figure 3) $\hat{H}^{m,+}_{1,\text{PFM}}$ and $\hat{H}^{m,+}_{3,\text{PFM}}$ behave similarly and $\hat{H}^{m,+}_{2,\text{PFM}}$ is slightly oversized for $N = 2, 3$. For $N = 5, 10, 20$ $\hat{H}^{m,+}_{2,\text{PFM}}$ and $\hat{H}^{m,+}_{3,\text{PFM}}$ work similarly, slightly above the chosen significance level, only $\hat{H}^{m,+}_{1,\text{PFM}}$ has a lower null rejection probabilty, closer to the significance level. In case of $N = 30$ $\hat{H}^{m,+}_{1,\text{PFM}}$ is closer to the significance level as $\hat{H}^{m,+}_{2,\text{PFM}}$ which is closer than $\hat{H}^{m,+}_{3,\text{PFM}}$. In all cases of N size distortions vanish for larger m.

3.2. Null Rejection Probability with Fixed Calibration Period

We looked at finite sample performance by fixing the combined calibration and monitoring period T and compared different sets of parameter values, e.g. the influence of m on the performance of the procedure. This is only helpful in a case of retrospective analysis where we have to specify this value ex post. In the practical case of having a data set and a stream of newly incoming data we cannot specify m a priori independently of T. Merely, we have an assumed to be break free calibration period of a fixed length $[mT]$. Thus, we need to figure out how to specify m and T jointly since there are, in principle, uncountably infinite combinations possible.

In this scenario we simulated under (40) and (41) for $t = 1, \ldots, T$ and applied the detectors from Section 2.1. We fixed the value $[mT]$ and simulated time series using pairs (m, T) such that the length of the calibration period is constant displayed in Figures 4 and 5. The smaller m and consequently the larger T is, the better the performance is in the sense of small size distortion (level 5%). Larger values of T yield better approximations of the test statistics asymptotic distributions since the procedure is built on large T asymptotics and m is a fixed parameter. That means, we recommend choosing T as large as possible for monitoring newly incoming data.

3.3. Null Rejection Probability in Correlated Homogeneous Cointegrating Regressions

We abandon Assumption 4 of independent cointegrating regressions and consider the detectors from Sections 2.2 and 2.3 based on PFM-GLS and FM-SUR estimation, respectively. We use a data generating process that has a similar covariance and long-run
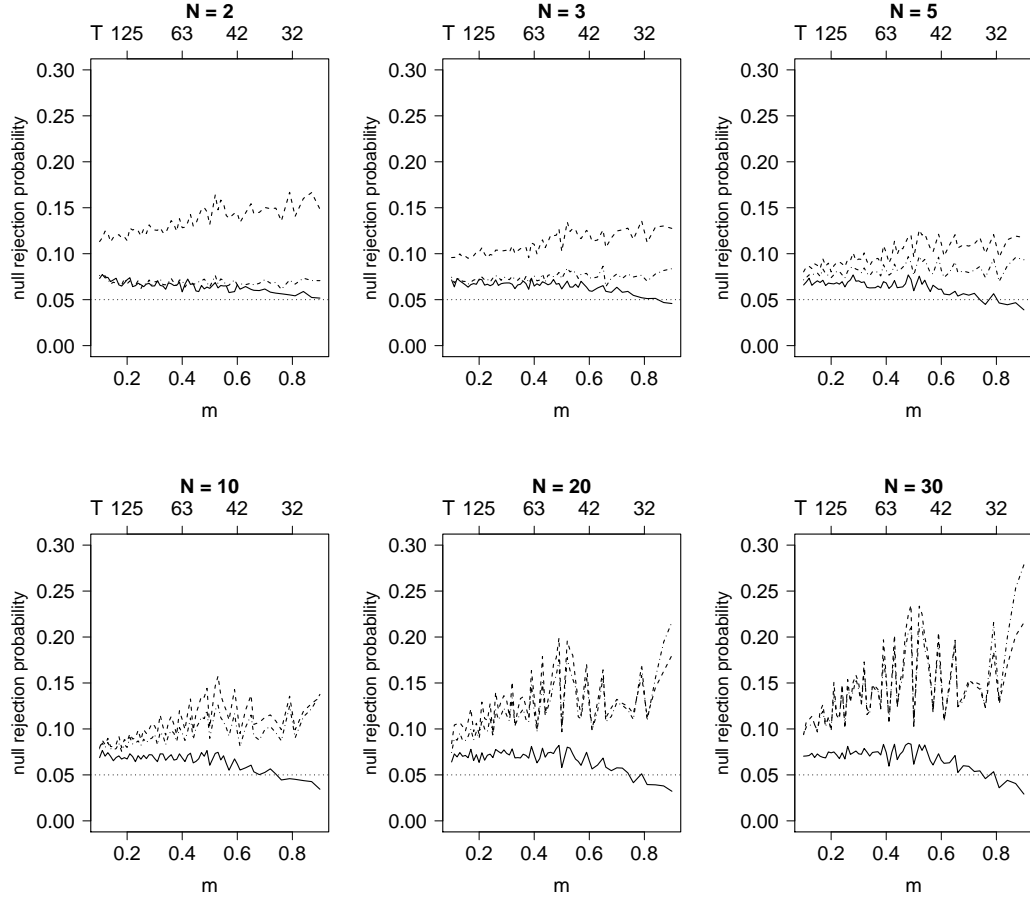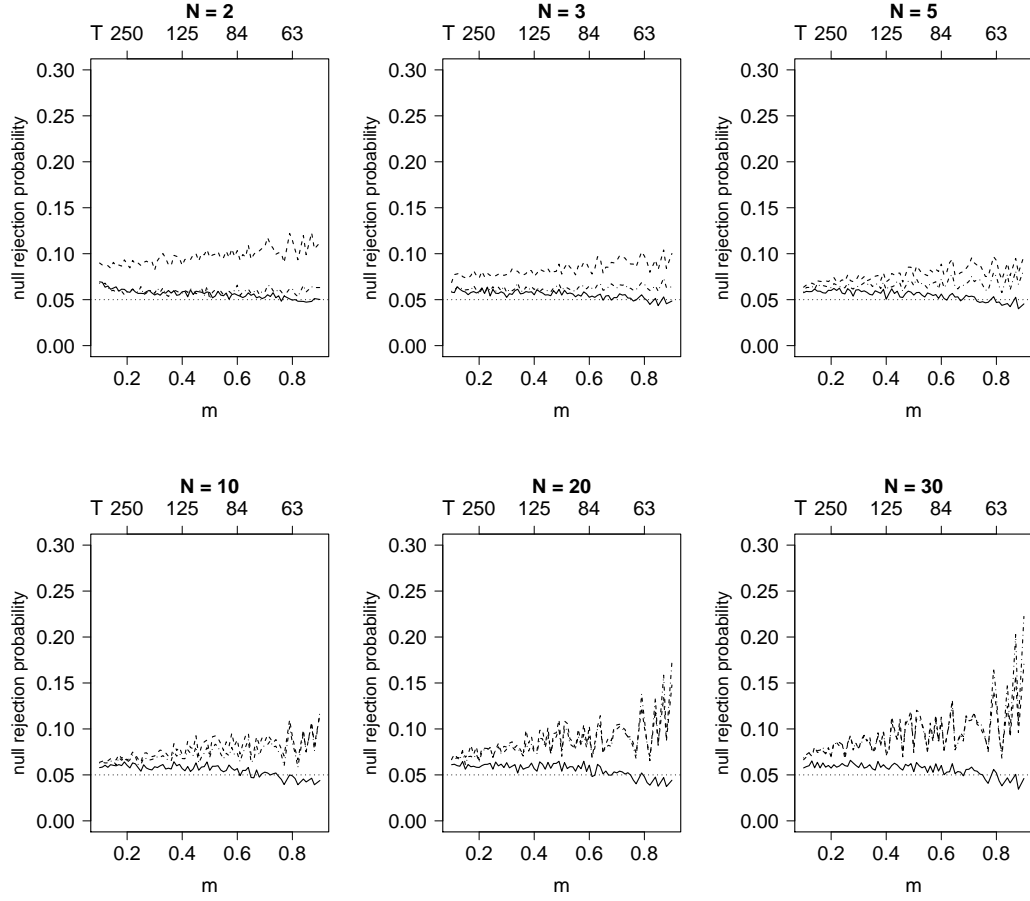
Figure 4: Null rejection probability with a fixed calibration period (Section 3.2) with $[mT] = 25$, $\rho_1 = \rho_2 = 0.3$ and PFM-OLS estimation. The lines represent $\hat{H}_{1,\mathrm{PFM}}^{m,+}$ (solid), $\hat{H}_{2,\mathrm{PFM}}^{m,+}$ (dashed) and $\hat{H}_{3,\mathrm{PFM}}^{m,+}$ (dotdashed).

Figure 5: Null rejection probability with a fixed calibration period (Section 3.2) with $[mT] = 50$, $\rho_1 = \rho_2 = 0.3$ and PFM-OLS estimation. The lines represent $\hat{H}_{1,\mathrm{PFM}}^{m,+}$ (solid), $\hat{H}_{2,\mathrm{PFM}}^{m,+}$ (dashed) and $\hat{H}_{3,\mathrm{PFM}}^{m,+}$ (dotdashed).

covariance structure as the data in the application section, namely

$$y_{n,t} = \mu + x_{n,t,1}\beta_1 + x_{n,t,2}\beta_2 + u_{n,t},$$
$$x_{n,t,i} = x_{n,t-1,i} + v_{n,t,i}, \quad x_{n,0,i} = 0, \quad i = 1, 2, \tag{42}$$

where

$$u_{n,t} = \rho_1 u_{n,t-1} + (\varepsilon_{n,t} + \rho_2(e_{n,t,1} + e_{n,t,2}))/10, \quad u_{n,0} = 0,$$
$$v_{n,t,i} = (e_{n,t,i} + 0.5 e_{n,t-1,i} + 0.25 e_{n,t-2,i})/10^{3/2}, \quad i = 1, 2, \tag{43}$$

for $t = 1, \ldots, [mT]$. $\varepsilon_{n,t}$ is an i.i.d. standard normal random variable independent of $e_t = [e_{1,t,1}, e_{1,t,2}, e_{2,t,1}, \ldots e_{N,t,2}]'$. e_t is serially independent and follows a multivariate normal distribution with expected value 0 and covariance matrix $\mathrm{Cov}(e_t) = (1 - \tilde{\rho})\mathbf{I_N} + \tilde{\rho}\mathbf{1_{N \times N}}$, where $\mathbf{1_{N \times N}}$ is the $N \times N$ matrix of ones. $\tilde{\rho}$ controls the instantaneous correlation among regressors $v_{n,t}$ and error term $u_{n,t}$ for a single cointegrating regression as well as the instantaneous correlation of regressors and error terms in the cross-section dimension. Further, it holds that $\Omega_{uu} = (1-\rho_1)^{-2}((1+2\rho_2^2(1+\tilde{\rho})-4\tilde{\rho}\rho_2^2)\mathbf{I_N}+4\tilde{\rho}\rho_2^2\mathbf{1_{N \times N}})10^{-2}, \Omega_{vv} = 3.0625((1 - \tilde{\rho})\mathbf{I_{kN}} + \tilde{\rho}\mathbf{1_{kN \times kN}})10^{-3}$ and $\Omega_{uv} = 1.75\rho_2(1 - \rho_1)^{-1}((1 - \tilde{\rho})\mathbf{I_k} \otimes \mathbf{1_{1 \times N}} + 2\tilde{\rho}\mathbf{1_{N \times kN}})10^{-5/2}$. We choose $\mu = 3$ and $\beta_1 = \beta_2 = 1$ again as well as $\tilde{\rho} = 0.9$. The errors are scaled such that they mimic the magnitude and covariance structure of the errors in the application in Section 4.

This data generating process violates the assumption of independence across cointegrating relations. By allowing for cross-sectional dependence and heterogeneous (co-)variances the number of additional long-run variance parameters increases from $\frac{1}{2}(k + 1)(k + 2)$ to $\frac{1}{2}(N + 1)k((N + 1)k + 1)$. S feasible simplification to reduce the number of parameters for large values of N or k is to assume homogeneous long-run variances across $u_{n,t}$ and homogeneous long-run variances across $v_{n,t,i}$. Further, assuming $\Omega_{uu}^{i,j} = \Omega_{uu}^{h,l}$, $\Omega_{uv}^{i,j} = \Omega_{uv}^{h,l}$, $\Omega_{uv}^{i,i} = \Omega_{uv}^{h,h}$, $\Omega_{vv}^{i,j} = \Omega_{vv}^{h,l}$ and $\Omega_{vv}^{i,i} = \Omega_{vv}^{h,h}$ for $i \neq j, h \neq l \in \{1, \ldots, N\}$ results in $\frac{1}{2}(3k^2 + 5k + 4)$ parameters to be estimated. We realize the estimation of the simplified long-run variance structure for $N > 2$ by pairwisely estimating the long-run variance of all bivariate systems of cointegrating regressions $n_1, n_2 \in \{1, \ldots, N\}$ and averaging over all possible pairs.

Figures 6 and 7 display the null rejection probability for $T = 500$, $\rho_1 = \rho_2 = 0.3, 0.6$, $\tilde{\rho} = 0.9$ and $N \in \{2, 3, 5, 10, 20, 30\}$ of the detectors based on PFM-GLS and FM-SUR estimation. We focus on the detectors which have reasonable empirical sizes. The size distortions are larger than in the case of the PFM-OLS estimator and they depend on
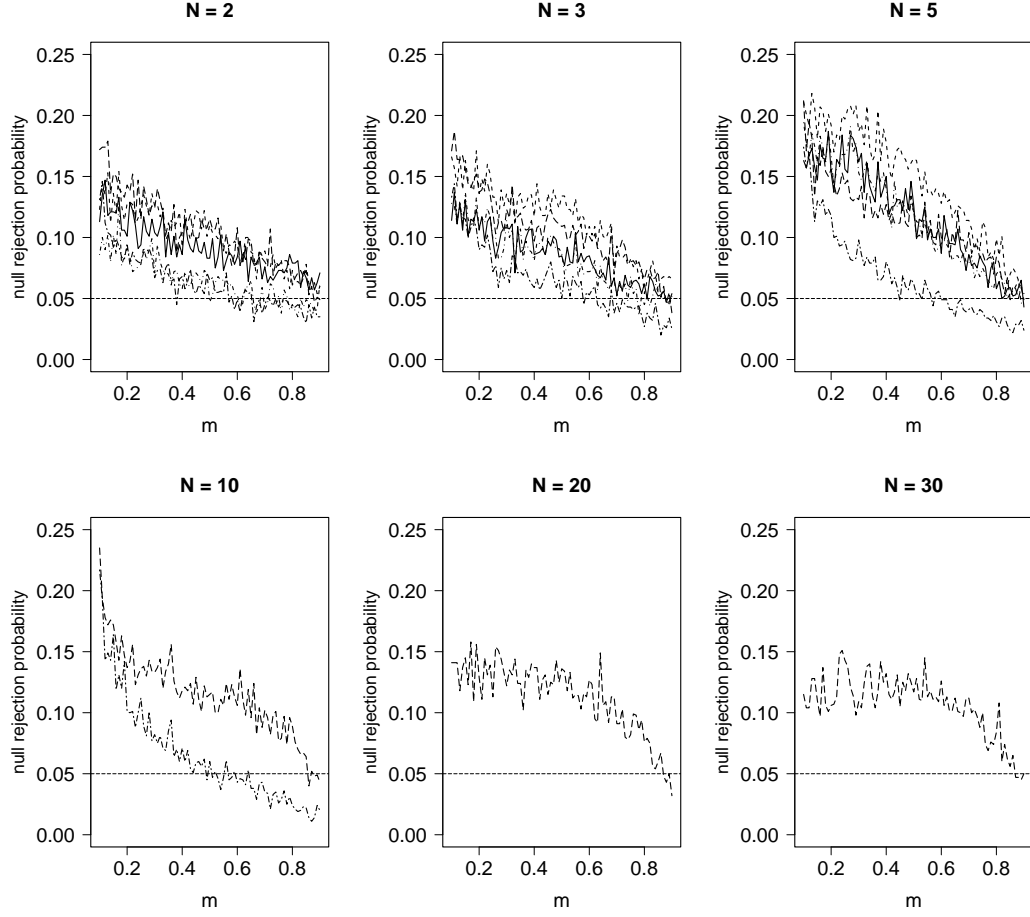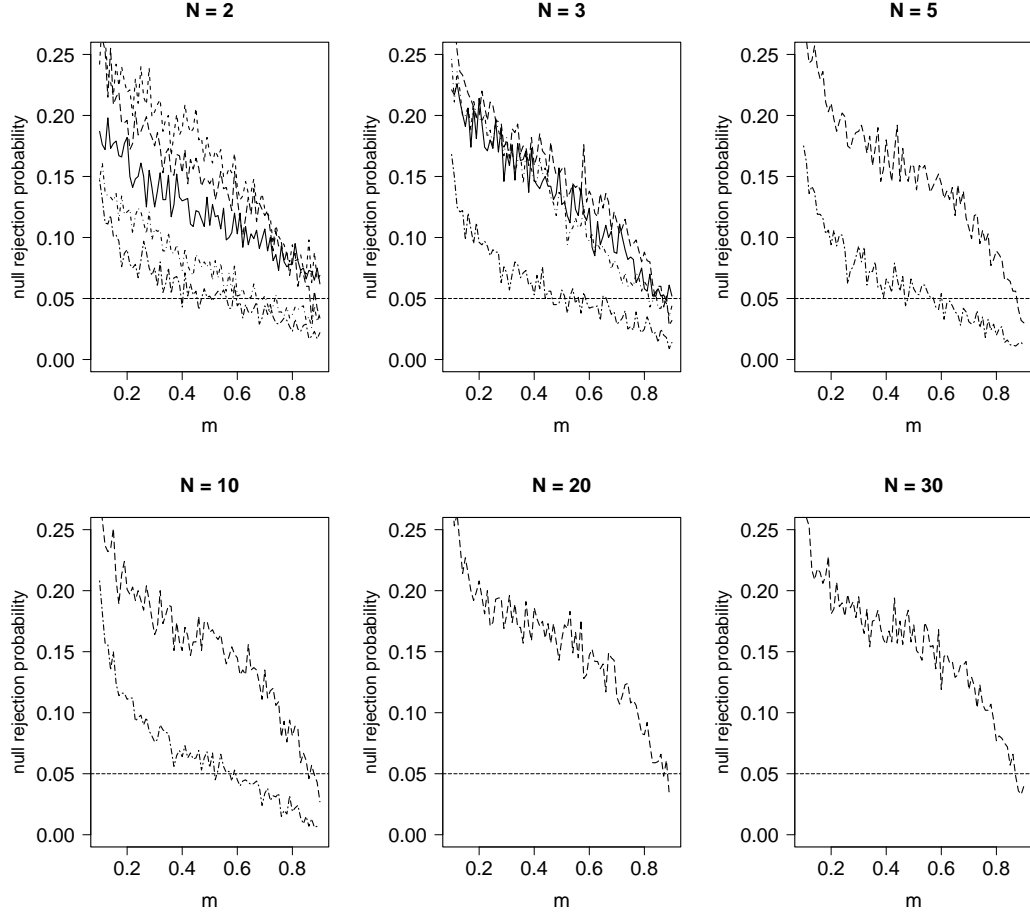
Figure 6: Null rejection probability in correlated homogeneous cointegrating regressions (Section 3.3) with $T = 500$, $\rho_1 = \rho_2 = 0.3$, $\tilde{\rho} = 0.9$ and PFM-GLS and FM-SUR estimation. The lines represent $\hat{H}^{m,+}_{1,\text{PFM-GLS}}$ (solid), $\hat{H}^{m,+}_{2,\text{PFM-GLS}}$ (dashed), $\hat{H}^{m,+}_{3,\text{PFM-GLS}}$ (dotdashed), $\hat{H}^{m,+}_{2,\text{FM-SUR}}$ (long-dashed) and $\hat{H}^{m,+}_{3,\text{FM-SUR}}$ (two-dashed).

Figure 7: Null rejection probability in correlated homogeneous cointegrating regressions (Section 3.3) with $T = 500$, $\rho_1 = \rho_2 = 0.6$, $\tilde{\rho} = 0.9$ and PFM-GLS and FM-SUR estimation. The lines represent $\hat{H}^{m,+}_{1,\text{PFM-GLS}}$ (solid), $\hat{H}^{m,+}_{2,\text{PFM-GLS}}$ (dashed), $\hat{H}^{m,+}_{3,\text{PFM-GLS}}$ (dotdashed), $\hat{H}^{m,+}_{2,\text{FM-SUR}}$ (long-dashed) and $\hat{H}^{m,+}_{3,\text{FM-SUR}}$ (two-dashed).

Table 2: Power in uncorrelated homogeneous cointegrating regressions (Section 3.4) with $T = 100$, $\rho_1 = \rho_2 = 0.3$, $N = 5$ and PFM-OLS estimation. The number of breaks is 2 in the first six rows and 4 in the last six rows.

breaks			$\hat{H}_{1,\mathrm{PFM}}^{m,+}$	$\hat{H}_{2,\mathrm{PFM}}^{m,+}$	$\hat{H}_{3,\mathrm{PFM}}^{m,+}$
	$m = 0.25$	$r = 0.25$	0.52	0.72	0.58
		$r = 0.50$	0.30	0.41	0.26
2		$r = 0.75$	0.13	0.13	0.09
	$m = 0.50$	$r = 0.50$	0.85	0.93	0.86
		$r = 0.75$	0.59	0.65	0.32
	$m = 0.75$	$r = 0.75$	0.91	0.93	0.85
	$m = 0.25$	$r = 0.25$	0.77	0.92	0.82
		$r = 0.50$	0.47	0.65	0.43
4		$r = 0.75$	0.21	0.20	0.11
	$m = 0.50$	$r = 0.50$	0.97	1.00	0.97
		$r = 0.75$	0.83	0.87	0.54
	$m = 0.75$	$r = 0.75$	0.99	1.00	0.97

which particular estimator is used. The size curves show the interesting pattern that the empirical size declines linearly in m. To some extent, this effect could be expected due to the necessity to estimate nuisance parameters. Still, we believe that the detectors are useful as the size distortions are moderate.

3.4. Power under Slope Breaks in Uncorrelated Homogeneous Cointegrating Regressions

Now, we turn to power evaluation under slope breaks by which we mean a change in the parameters β_1 or β_2. We consider the detectors from Section 2.1 and simulate under (40) and (41) for $t = 1, \ldots, [rT]$ and from $[rT] + 1$ on a subset of the parameters in (40) changes. More precisely, there is a break in a different number of the cointegrating relationships and β_1 and β_2 change to $\beta_{1,n} = \beta_{2,n} = 1 - \delta$ in the first half of the breaking cointegrating relationships and change to $\beta_{1,n} = \beta_{2,n} = 1 + \delta$ in the second half with $\delta = 0.05$. Thus, the system is no longer homogeneous after the structural break. Note that we consider $T = 100$ under this alternative as the power is 1 in almost all the cases we study below for $T = 500$ (as under the null hypothesis).

In Table 2, we see that $\hat{H}_{2,\mathrm{PFM}}^{m,+}$ has higher power than the other detectors except for the case $m = 0.25, r = 0.5$ and two breaks ($\hat{H}_{1,\mathrm{PFM}}^{m,+}$ has higher power) and for the case $m = 0.25, r = 0.75$ and four breaks ($\hat{H}_{1,\mathrm{PFM}}^{m,+}$ has higher power). Keeping in mind that $\hat{H}_{2,\mathrm{PFM}}^{m,+}$ has higher size distortions than $\hat{H}_{1,\mathrm{PFM}}^{m,+}$ and $\hat{H}_{3,\mathrm{PFM}}^{m,+}$ this is no surprise. In general,

Table 3: Power in uncorrelated homogeneous cointegrating regressions (Section 3.4) with $T = 100$, $\rho_1 = \rho_2 = 0.3$, $N = 10$ and PFM-OLS estimation. The number of breaks is 2 in the first six rows and $4, 6, 8, 10$ for each of the following six rows.

breaks			$\hat{H}^{m,+}_{1,\text{PFM}}$	$\hat{H}^{m,+}_{2,\text{PFM}}$	$\hat{H}^{m,+}_{3,\text{PFM}}$
	$m = 0.25$	$r = 0.25$	0.70	0.78	0.72
		$r = 0.50$	0.42	0.44	0.35
		$r = 0.75$	0.17	0.13	0.10
2	$m = 0.50$	$r = 0.50$	0.93	0.94	0.90
		$r = 0.75$	0.72	0.63	0.41
	$m = 0.75$	$r = 0.75$	0.93	0.90	0.82
	$m = 0.25$	$r = 0.25$	0.94	0.97	0.95
		$r = 0.50$	0.70	0.73	0.61
		$r = 0.75$	0.28	0.18	0.11
4	$m = 0.50$	$r = 0.50$	1.00	1.00	0.99
		$r = 0.75$	0.94	0.88	0.65
	$m = 0.75$	$r = 0.75$	1.00	0.99	0.97
	$m = 0.25$	$r = 0.25$	0.99	1.00	0.99
		$r = 0.50$	0.86	0.90	0.78
		$r = 0.75$	0.43	0.26	0.13
6	$m = 0.50$	$r = 0.50$	1.00	1.00	1.00
		$r = 0.75$	0.99	0.97	0.82
	$m = 0.75$	$r = 0.75$	1.00	1.00	1.00
	$m = 0.25$	$r = 0.25$	1.00	1.00	1.00
		$r = 0.50$	0.94	0.96	0.89
		$r = 0.75$	0.54	0.35	0.15
8	$m = 0.50$	$r = 0.50$	1.00	1.00	1.00
		$r = 0.75$	1.00	0.99	0.91
	$m = 0.75$	$r = 0.75$	1.00	1.00	1.00
	$m = 0.25$	$r = 0.25$	1.00	1.00	1.00
		$r = 0.50$	0.97	0.98	0.94
		$r = 0.75$	0.65	0.43	0.18
10	$m = 0.50$	$r = 0.50$	1.00	1.00	1.00
		$r = 0.75$	1.00	1.00	0.96
	$m = 0.75$	$r = 0.75$	1.00	1.00	1.00

Table 4: Power in uncorrelated homogeneous cointegrating regressions (Section 3.5) with $T = 100$, $\rho_1 = \rho_2 = 0.3$, $N = 5$ and PFM-OLS estimation. The number of breaks is 1 in the first six rows and $2, 3, 4, 5$ for each of the following six rows.

breaks			$\hat{H}_{1,\mathrm{PFM}}^{m,+}$	$\hat{H}_{2,\mathrm{PFM}}^{m,+}$	$\hat{H}_{3,\mathrm{PFM}}^{m,+}$
	$m = 0.25$	$r = 0.25$	0.47	0.59	0.45
		$r = 0.50$	0.20	0.24	0.15
1		$r = 0.75$	0.08	0.10	0.08
	$m = 0.50$	$r = 0.50$	0.66	0.76	0.59
		$r = 0.75$	0.23	0.23	0.10
	$m = 0.75$	$r = 0.75$	0.58	0.61	0.38
	$m = 0.25$	$r = 0.25$	0.71	0.84	0.71
		$r = 0.50$	0.32	0.41	0.24
2		$r = 0.75$	0.10	0.10	0.08
	$m = 0.50$	$r = 0.50$	0.87	0.94	0.85
		$r = 0.75$	0.41	0.41	0.17
	$m = 0.75$	$r = 0.75$	0.81	0.84	0.62
	$m = 0.25$	$r = 0.25$	0.83	0.94	0.85
		$r = 0.50$	0.44	0.54	0.30
3		$r = 0.75$	0.10	0.10	0.07
	$m = 0.50$	$r = 0.50$	0.96	0.99	0.93
		$r = 0.75$	0.52	0.54	0.20
	$m = 0.75$	$r = 0.75$	0.91	0.93	0.75
	$m = 0.25$	$r = 0.25$	0.90	0.98	0.91
		$r = 0.50$	0.52	0.64	0.38
4		$r = 0.75$	0.12	0.12	0.09
	$m = 0.50$	$r = 0.50$	0.99	1.00	0.97
		$r = 0.75$	0.65	0.67	0.27
	$m = 0.75$	$r = 0.75$	0.97	0.98	0.86
	$m = 0.25$	$r = 0.25$	0.95	0.99	0.95
		$r = 0.50$	0.60	0.73	0.44
5		$r = 0.75$	0.15	0.13	0.09
	$m = 0.50$	$r = 0.50$	1.00	1.00	0.99
		$r = 0.75$	0.74	0.76	0.33
	$m = 0.75$	$r = 0.75$	0.99	0.99	0.91

power is higher in the case $m = r$ than in the case $m < r$, i.e. the monitoring works most succesfully when the structural break occurs directly after the end of the calibration period. Between $\hat{H}_{1,\text{PFM}}^{m,+}$ and $\hat{H}_{3,\text{PFM}}^{m,+}$ there is no clear ranking visible regarding power in this scenario.

Table 3 underlines that in most cases $\hat{H}_{2,\text{PFM}}^{m,+}$ has the highest power. The weakness of this detector lies in the case $m = 0.25, r = 0.75$ (or generally in breaks "long" after the calibration period). In this case, $\hat{H}_{1,\text{PFM}}^{m,+}$ has higher power than $\hat{H}_{2,\text{PFM}}^{m,+}$ and $\hat{H}_{3,\text{PFM}}^{m,+}$. All detectors get higher power for higher breakpoint counts where $\hat{H}_{3,\text{PFM}}^{m,+}$ has the worst performance.

3.5. Power and Detection Time under Breaks in Uncorrelated Homogeneous Cointegrating Regressions

In this scenario, we consider the detectors from Section 2.1 and (40) holds for $t = 1, \ldots, T$ and (41) holds for $t = 1, \ldots, [rT]$ where the parameter ρ_1 changes to $\rho_1 = 1$ from $t = [rT] + 1$ on for a subset of the cointegrating relationships. Thus, a fraction of the error processes $\{u_{n,t}\}_{t=[rT]+1,\ldots,T}$ are random walks and, therefore, the corresponding cointegrating relationships are no longer valid.

In Table 4 $\hat{H}_{2,\text{PFM}}^{m,+}$ has the highest power in most cases, $\hat{H}_{1,\text{PFM}}^{m,+}$ and $\hat{H}_{3,\text{PFM}}^{m,+}$ behave similarly with some exceptions where $\hat{H}_{3,\text{PFM}}^{m,+}$ has substantially less power. Overall, $\hat{H}_{1,\text{PFM}}^{m,+}$ has power not far off $\hat{H}_{2,\text{PFM}}^{m,+}$ and keeping in mind the size distortions of $\hat{H}_{2,\text{PFM}}^{m,+}$ makes $\hat{H}_{1,\text{PFM}}^{m,+}$ favourable. In general, the power is higher for a higher number of cointegrating relationships with breaks. A weakness lies in the case $m = 0.25$ and $r = 0.75$ where the power is low.

In Table 5 we display the mean detection delay conditional on detecting a break point and see that the detection delay is negative in most cases of $m = 0.25$ and $r = 0.75$, suggesting that a lot of false alarms in comparison to correct alarms occur in this case. The negative delays get closer to 0 when the number of breaks is greater indicating that the rate of correct alarms gets higher. The detection delay declines in m with the exception of $m = 0.25, r = 0.75$. Note that the detection delay is bounded by $(m - r)T$ and $(1 - r)T$. The smaller detection delay in the case $m = r = 0.75$ is not contributed to the fact that there are fewer observations left in this case than in the case $m = r = 0.25$ because we see in Table 4 that the power is nearly identical in the two cases. Overall, we can say the more breaks occur the smaller the detection delay is. When $m < r$ the detection delay is lower but the power is substantially lower as well. In almost all cases

Table 5: Mean detection delay in uncorrelated homogeneous cointegrating regressions (Section 3.5) provided the monitoring procedure detects a break point with $T = 100$, $\rho_1 = \rho_2 = 0.3$, $N = 5$ and PFM-OLS estimation. The number of breaks is 1 in the first six rows and $2, 3, 4, 5$ for each of the following six rows.

breaks			$\hat{H}^{m,+}_{1,\text{PFM}}$	$\hat{H}^{m,+}_{2,\text{PFM}}$	$\hat{H}^{m,+}_{3,\text{PFM}}$
1	$m = 0.25$	$r = 0.25$	24.74	26.48	32.17
		$r = 0.50$	21.32	25.44	24.68
		$r = 0.75$	-15.77	-8.77	-10.71
	$m = 0.50$	$r = 0.50$	20.87	22.01	27.82
		$r = 0.75$	12.30	14.51	12.00
	$m = 0.75$	$r = 0.75$	13.44	16.25	17.89
2	$m = 0.25$	$r = 0.25$	21.22	21.60	28.77
		$r = 0.50$	21.09	27.28	27.14
		$r = 0.75$	-10.17	-5.11	-9.94
	$m = 0.50$	$r = 0.50$	17.19	17.46	24.84
		$r = 0.75$	13.16	15.12	13.13
	$m = 0.75$	$r = 0.75$	11.73	13.54	17.08
3	$m = 0.25$	$r = 0.25$	18.30	17.40	25.77
		$r = 0.50$	23.26	27.14	29.28
		$r = 0.75$	-5.21	-3.72	-10.40
	$m = 0.50$	$r = 0.50$	14.04	14.51	22.23
		$r = 0.75$	13.51	15.63	15.35
	$m = 0.75$	$r = 0.75$	10.58	12.38	16.53
4	$m = 0.25$	$r = 0.25$	16.11	15.36	23.76
		$r = 0.50$	23.14	26.64	29.31
		$r = 0.75$	-3.46	-2.58	-5.62
	$m = 0.50$	$r = 0.50$	12.43	12.61	20.44
		$r = 0.75$	13.20	15.26	15.69
	$m = 0.75$	$r = 0.75$	9.39	11.29	15.84
5	$m = 0.25$	$r = 0.25$	14.22	12.60	20.79
		$r = 0.50$	22.25	26.12	29.64
		$r = 0.75$	1.05	-1.20	-5.14
	$m = 0.50$	$r = 0.50$	10.63	11.25	18.82
		$r = 0.75$	12.67	14.94	16.26
	$m = 0.75$	$r = 0.75$	8.34	10.38	15.13

$\hat{H}_{1,\text{PFM}}^{m,+}$ has a smaller detection delay than $\hat{H}_{2,\text{PFM}}^{m,+}$ and $\hat{H}_{3,\text{PFM}}^{m,+}$. There is no clear ranking between $\hat{H}_{2,\text{PFM}}^{m,+}$ and $\hat{H}_{3,\text{PFM}}^{m,+}$ visible.

3.6. Power under Breaks in Correlated Homogeneous Cointegrating Regressions

We consider the detectors from Sections 2.2 and 2.3 based on PFM-GLS and FM-SUR estimation, respectively, and revisit the data generating process (42) for $t = 1, \ldots, T$ and (43) for $t = 1, \ldots, [rT]$ with cross-sectionally dependent errors. From $[rT] + 1$ onwards for a fraction of the cointegrating relationships the parameter ρ_1 changes to $\rho_1 = 1$ such that a fraction of the error processes $\{u_{n,t}\}_{t=[rT]+1,\ldots,T}$ are random walks.

We display our results in Table 6. The PFM-GLS detectors have higher power than the FM-SUR ones, but it should be kept in mind that the empirical size is also higher. Similarly as in the case of Table 4, the power is higher for a higher number of cointegrating relationships with breaks and the power is rather low for $m = 0.25$ and $r = 0.75$.

4. Application

We consider the cointegrating relation between triplets of logarithmic currency exchange rates. We computed exchange rates between Bitcoin and real-world non-cryptocurrencies (USD, EUR, AUD, RUB, etc.) and perform three distinct bivariate analyses meaning that we consider two cointegrating relationships a time. In the analysis, we first consider the detectors from Section 2.1. There is statistical evidence that the assumption of cross-sectional independence is not fulfilled, but simulations for robustness using the same data generating process as in Section 3.3 indicate that it might still be appropriate to use these detectors (see Appendix C). Under the assumption of cross-sectional dependence, we could use the detectors from Section 2.2 and 2.3, but would have to estimate additional parameters. Nevertheless, we run the analysis also for the other estimators and observed slightly different results which are also presented.

We use our methods to simultaneously search for instabilities in multiple parities and to our best knowledge there exists no such analysis in the literature, yet. Other authors only consider one currency triplet at a time and therefore just one cointegrating regression. We assume violations of triangular arbitrage parity under normal market conditions to be stationary and a turn to non-stationary deviations or a change in parameters is a sign of mispricing not due to financial frictions – also referred to as financial market

Table 6: Power in correlated homogeneous cointegrating regressions (Section 3.6) with $T = 200$, $\rho_1 = \rho_2 = 0.3$, $\tilde{\rho} = 0.9$, $N = 5$ and PFM-GLS and FM-SUR estimation. The number of breaks is 1 in the first six rows and $2, 3, 4, 5$ for each of the following six rows.

breaks			$\hat{H}^{m,+}_{1,\text{PFM-GLS}}$	$\hat{H}^{m,+}_{2,\text{PFM-GLS}}$	$\hat{H}^{m,+}_{3,\text{PFM-GLS}}$	$\hat{H}^{m,+}_{2,\text{FM-SUR}}$	$\hat{H}^{m,+}_{3,\text{FM-SUR}}$
	$m = 0.25$	$r = 0.25$	0.86	0.90	0.81	0.68	0.48
		$r = 0.50$	0.69	0.72	0.55	0.44	0.25
1		$r = 0.75$	0.35	0.31	0.21	0.21	0.14
	$m = 0.50$	$r = 0.50$	0.90	0.94	0.84	0.81	0.59
		$r = 0.75$	0.60	0.62	0.34	0.34	0.11
	$m = 0.75$	$r = 0.75$	0.79	0.79	0.62	0.80	0.55
	$m = 0.25$	$r = 0.25$	0.97	0.98	0.96	0.89	0.70
		$r = 0.50$	0.88	0.90	0.75	0.63	0.32
2		$r = 0.75$	0.47	0.36	0.22	0.24	0.15
	$m = 0.50$	$r = 0.50$	0.99	1.00	0.97	0.97	0.85
		$r = 0.75$	0.84	0.84	0.51	0.56	0.20
	$m = 0.75$	$r = 0.75$	0.96	0.96	0.85	0.96	0.79
	$m = 0.25$	$r = 0.25$	0.99	1.00	0.99	0.97	0.84
		$r = 0.50$	0.95	0.97	0.88	0.74	0.41
3		$r = 0.75$	0.56	0.46	0.25	0.22	0.15
	$m = 0.50$	$r = 0.50$	1.00	1.00	0.99	1.00	0.94
		$r = 0.75$	0.94	0.92	0.61	0.70	0.25
	$m = 0.75$	$r = 0.75$	0.99	0.99	0.94	0.99	0.90
	$m = 0.25$	$r = 0.25$	1.00	1.00	1.00	0.99	0.91
		$r = 0.50$	0.98	0.99	0.94	0.84	0.48
4		$r = 0.75$	0.67	0.56	0.26	0.25	0.13
	$m = 0.50$	$r = 0.50$	1.00	1.00	1.00	1.00	0.96
		$r = 0.75$	0.97	0.96	0.69	0.81	0.27
	$m = 0.75$	$r = 0.75$	1.00	1.00	0.97	1.00	0.96
	$m = 0.25$	$r = 0.25$	1.00	1.00	1.00	1.00	0.94
		$r = 0.50$	0.99	1.00	0.96	0.89	0.53
5		$r = 0.75$	0.75	0.63	0.28	0.27	0.16
	$m = 0.50$	$r = 0.50$	1.00	1.00	1.00	1.00	0.99
		$r = 0.75$	0.98	0.99	0.81	0.87	0.34
	$m = 0.75$	$r = 0.75$	1.00	1.00	0.98	1.00	0.98

dislocation. We find empirical evidence of such mispricing in currency triplets including Bitcoin and use our results in a portfolio trading strategy.

Financial market dislocations are difficult to define and measure, yet arbitrage parities are a less controversial matter (Pasquariello, 2014) and were investigated, for instance, by Yu and Zhang (2017) with a focus on Bitcoin and the relationship between triangular arbitrage parity deviations and cross-country differences in capital controls which can be linked to different demand on foreign currency across countries. Corbet et al. (2018) link Bitcoin prices to fundamentals that seem to drive the price until 2017; after that their model signals bubble-type behaviour. Such bubble-type behaviour can be modeled using the theory of Cretarola and Figà-Talamanca (2021). Cheah and Fry (2015) link Bitcoin prices to fundamentals as well, show that Bitcoin prices are prone to speculative bubbles and find empirical evidence that the fundamental price of Bitcoin is zero; Dong and Dong (2014) conclude that Bitcoin is an immature currency; and Lintilhac and Tourin (2017) use Bitcoin to construct portfolio strategies. Reynolds et al. (2021) investigate the time series properties of Bitcoin and fiat currency logarithmic exchange rates. Their findings suggest these are unit root processes and they consider univariate cointegrating relationships between triplets of logarithmic currency exchange rates. They present empirical evidence of mispricings in currency triplets including Bitcoin investigating one cointegrating relation at a time and use their result for a currency portfolio strategy.

The law of one price is implied by the assumptions of arbitrage-free markets in modern financial theory meaning prices of related assets are fundamentally linked and should inhibit arbitrage parities. Consider a currency triplet (A-V-B) consisting of three currencies A, B and V (the vehicle currency). Let $S_{A/B,t}$ denote the units of currency A received for one unit of currency B. In the absence of arbitrage, for any triplet of spot exchange rates the triangular arbitrage parity

$$S_{A/B,t} = S_{A/V,t} S_{V/B,t} \quad \Leftrightarrow \quad \ln S_{A/B,t} = \ln S_{A/V,t} + \ln S_{V/B,t} \tag{44}$$

holds. In real data we never observe the validity of (44). This is suspectedly due to market frictions such as transactions cost. In order to compensate for these frictions we include a stationary error term in (44) and assume that deviations from triangular arbitrage parity are stationary transforming (44) to

$$\ln S_{A/B,t} = \ln S_{A/V,t} + \ln S_{V/B,t} + u_t, \tag{45}$$

where u_t is the stationary error due to market frictions.

Currency triplets sharing more than one currency imply identical regressors and therefore we cannot apply our monitoring procedures: On the one hand, cross-sectional independence would be outruled by construction, on the other hand, a fixed correlation of one would not allow for simplifying the estimator of the long-run variance as described in Section 3.3. We consider three examples of two currency triplets a time with Bitcoin (XBT) as vehicle currency V in every triplet. US Dollar (USD) and Euro (EUR) are fixed currencies in each of the two triplets while the third currency varies among Australian Dollar (AUD), Canadian Dollar (CAD), Pound Sterling (GBP), Russian Ruble (RUB) and Swedish Krona (SEK). This choice is motivated by the fact that USD and EUR can be considered as global leading currencies from large economies and that the chosen currencies are most actively traded in our sample period. The triplets are (USD-XBT-CAD)–(EUR-XBT-GBP), (USD-XBT-SEK)–(GBP-XBT-EUR) and (USD-XBT-AUD)–(RUB-XBT-EUR).

We use daily spot exchange rates among fiat currencies as reported by the Pacific Exchange Rate Service (Bank of Canada, c.f. Antweiler, 2015).The exchange rates are the averages of transaction prices or price quotes from financial institutions between 11:59 a.m. and 12:02 p.m. Eastern time (ET). We use Bitcoin transaction prices between 11:59 a.m. and 12:01 p.m. ET as reported by Bitcoincharts (2017) to calculate noon exchange rates between Bitcoin and fiat currencies.

The chosen triplets leads to three bivariate systems of cointegrating relationships, namely

$$y_t = \begin{bmatrix} \ln S_{\text{USD/CAD},t} \\ \ln S_{\text{EUR/GBP},t} \end{bmatrix} = \begin{bmatrix} 1 & \ln S_{\text{USD/XBT},t} & \ln S_{\text{XBT/CAD},t} \\ 1 & \ln S_{\text{EUR/XBT},t} & \ln S_{\text{XBT/GBP},t} \end{bmatrix} \theta + u_t = X_t'\theta + u_t, \quad (46)$$

$$y_t = \begin{bmatrix} \ln S_{\text{USD/SEK},t} \\ \ln S_{\text{GBP/EUR},t} \end{bmatrix} = \begin{bmatrix} 1 & \ln S_{\text{USD/XBT},t} & \ln S_{\text{XBT/SEK},t} \\ 1 & \ln S_{\text{GBP/XBT},t} & \ln S_{\text{XBT/EUR},t} \end{bmatrix} \theta + u_t = X_t'\theta + u_t, \quad (47)$$

and

$$y_t = \begin{bmatrix} \ln S_{\text{USD/AUD},t} \\ \ln S_{\text{RUB/EUR},t} \end{bmatrix} = \begin{bmatrix} 1 & \ln S_{\text{USD/XBT},t} & \ln S_{\text{XBT/AUD},t} \\ 1 & \ln S_{\text{RUB/XBT},t} & \ln S_{\text{XBT/EUR},t} \end{bmatrix} \theta + u_t = X_t'\theta + u_t, \quad (48)$$

where $\theta = [0, 1, 1]'$ in each of them. The homogeneity of these three systems is a direct consequence of the triangular arbitrage parities.

The sample ranges from 1 May 2013 until 31 December 2015 due to high Bitcoin trading frequency and thus more reliable Bitcoin prices in this time frame, leading to a small $N = 2$, large $T = 667$ setting. We choose $m = 0.2$, i.e. calibration until 8 November 2013,

in order to have a rather small calibration period, compare the discussion after equation (4), and assume the cointegrating relation to be break free due to rather stable Bitcoin prices. For a further discussion of this matter the reader is referred to Reynolds et al. (2021). They investigate the time series properties of logarithmic Bitcoin exchange rates and demonstrate that logarithmic exchange rates including Bitcoin behave like I(1) processes. They perform unit root tests (Augmented-Dickey-Fuller and Phillips-Perron) and the KPSS test on logarithmic exchange rates including Bitcoin indicating that they indeed have a unit root. Furthermore, they perform the same tests on the series of first differences illustrating that these can be assumed to be stationary. For logarithmic exchange rates among fiat currencies I(1) behaviour is well established in the literature. For monitoring we apply $\hat{H}_{1,\text{PFM}}^{m,+}, \hat{H}_{2,\text{PFM}}^{m,+}$ and $\hat{H}_{3,\text{PFM}}^{m,+}$ for the PFM-OLS-case, $\hat{H}_{1,\text{PFM-GLS}}^{m,+}$, $\hat{H}_{2,\text{PFM-GLS}}^{m,+}$ and $\hat{H}_{3,\text{PFM-GLS}}^{m,+}$ for the PFM-GLS-case and $\hat{H}_{2,\text{FM-SUR}}^{m,+}$ and $\hat{H}_{3,\text{FM-SUR}}^{m,+}$ for the FM-SUR-case. In all cases, we use $D_t = 1$ and $g(s)$ according to Table 1. We detect structural breaks in all three pairs of currency triplets (c.f. Table 7), whereas most breaks can be found for the second triple. Figure 8 displays the observed process of all test statistics for all triplets. Important dates for the Bitcoin and financial market during our monitoring and prior to the detected breaks are the shut down of Mt. Gox, a Tokyo-based Bitcoin exchange, in February 2014 and the ending of the cap on euro-swiss franc exchange rates by the Swiss National Bank on 15 January 2015.

Given the entanglement of exchange rates the question of independent cointegrating regressions arises naturally. An application of Breusch and Pagan (1980) gives statistical evidence that the assumption of cross-sectional independence might not be reasonable. Similarly as in Section 3.3, we have conducted a robustness check investigating the

Table 7: Breakpoint detection dates in the three pairs of currency triplets

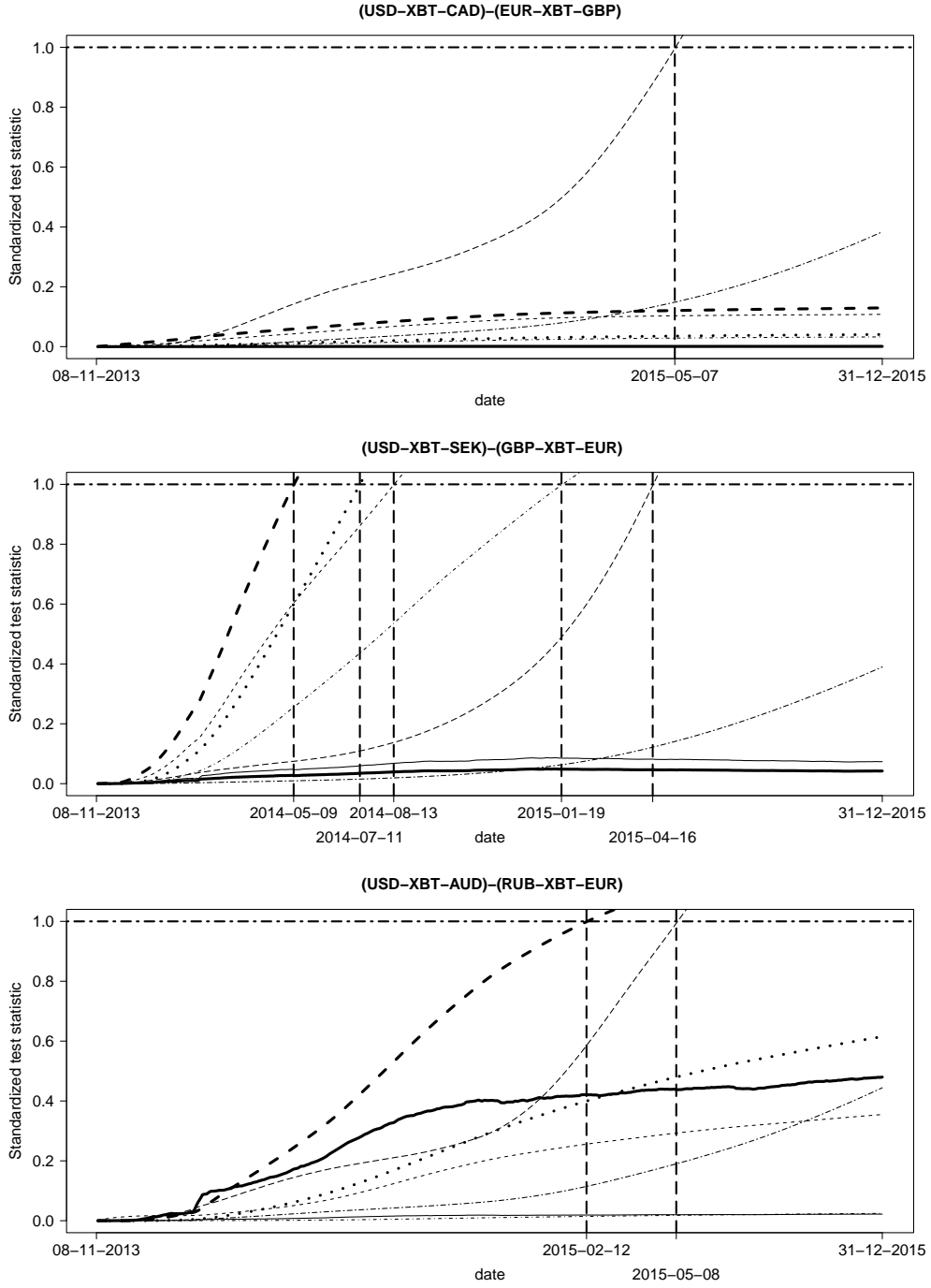|	(USD-XBT-CAD) (EUR-XBT-GBP)	(USD-XBT-SEK) (GBP-XBT-EUR)	(USD-XBT-AUD) (RUB-XBT-EUR)
$\hat{H}_{1,\text{PFM}}^{m,+}$	-	-	-
$\hat{H}_{2,\text{PFM}}^{m,+}$	-	09-05-2014	12-02-2015
$\hat{H}_{3,\text{PFM}}^{m,+}$	-	11-07-2014	-
$\hat{H}_{1,\text{PFM-GLS}}^{m,+}$	-	-	-
$\hat{H}_{2,\text{PFM-GLS}}^{m,+}$	-	13-08-2014	-
$\hat{H}_{3,\text{PFM-GLS}}^{m,+}$	-	19-01-2015	-
$\hat{H}_{2,\text{FM-SUR}}^{m,+}$	07-05-2015	16-04-2015	08-05-2015
$\hat{H}_{3,\text{FM-SUR}}^{m,+}$	-	-	-

Figure 8: Processes of the test statistics divided by the respective critical values are displayed for (46) - (48). Bold lines represent test statistics based on $\hat{H}_{1,\text{PFM}}^{m,+}$ (solid), $\hat{H}_{2,\text{PFM}}^{m,+}$ (dashed) and $\hat{H}_{3,\text{PFM}}^{m,+}$ (dotdashed), and non-bold lines represent test statistics based on $\hat{H}_{1,\text{PFM-GLS}}^{m,+}$ (solid), $\hat{H}_{2,\text{PFM-GLS}}^{m,+}$ (dashed), $\hat{H}_{3,\text{PFM-GLS}}^{m,+}$ (dotdashed), $\hat{H}_{2,\text{FM-SUR}}^{m,+}$ (long-dashed) and $\hat{H}_{3,\text{FM-SUR}}^{m,+}$ (two-dashed). The dashed vertical lines indicate the detected breakpoints in the respective systems of cointegrating relationships.

– 38–

PFM-OLS detectors for dependent cointegrating regressions of the form (42) and (43). It shows that the detectors work for $N = 2$ even under violation of the independence assumption and behave similarly to the PFM-GLS and FM-SUR detectors for $N = 2$ in this case. In the application examples, the long-run correlation among the first differences of the regressors of different cointegrating regressions $\Delta X_{1,t}$ and $\Delta X_{2,t}$ varies from 0.85 to 0.99 in absolute value and the longrun correlation in (43) is 0.9 among these first differences while the variances are of a similar magnitude of 0.0025 in the finite sample case and 0.004 to 0.006 in the application cases. The correlation between the errors $u_{1,t}$ and $u_{2,t}$ in the simulation is 0.2 while the estimated correlation in the applications is between 0.5 and 0.8. The correlations between the first differences of the regressors and the errors $u_{1,t}$ and $u_{2,t}$ vary beween 0.01 and 0.15 in the applications while they are roughly 0.5 in the simulation study. The longrun covariance and correlation matrices of the application examples and details about the econometric test for cross-sectional independence can be found in Appendix C.

We use our results to implement a portfolio trading strategy and compare, first, the three different pairs of triplets and, second, each of the different pairs to a benchmark portfolio using a simple buy-and-hold strategy. Each of the portfolios is equally-weighted among the five currencies included in a pair of currency triplets. USD serves as the domestic currency and we exchange one fifth of the portfolio volume to each of the four foreign currencies present in the respective pair of currency triplets at the start of monitoring on 12 November 2013. We assume that we earn the local risk free rate in each of the currencies which we proxy by the local deposit interest rate given by Euribor (European Money Markets Institute, 2020) as EUR deposit interest rate and LIBOR (Board of Governors of the Federal Reserve System, 2020) as USD deposit interest rate while we obtained AUD, CAD and RUB deposit interest rates from the World Bank (2020) and GBP and SEK deposit interest rates from the Bank of England (2020) and the Bank of Korea (2020), respectively.

The buy-and-hold benchmark portfolios hold the foreign currencies until the end of monitoring on 31 December 2015 and exchange them back to USD. The monitoring based portfolios exchange the foreign currencies back to USD on the detected breakdates and earn the local risk free USD rate until the end of monitoring. We neglect the effects of trading costs. In Table 8 we see that in case of the pair (USD-XBT-SEK)–(GBP-XBT-EUR) the monitoring based strategy achieves a substantial excess return compared to the benchmark strategy if we exchange back to USD on any of the first three breaks detected in 2014. Interestingly, trading back to USD on the later detected

Table 8: Returns of buy-and-hold strategy compared to monitoring based portfolio strategy for the three breakpoints

currency triplet	breakdate	benchmark return	excess return
(USD-XBT-CAD)	07-05-2015	−0.0655	−0.0713
(EUR-XBT-GBP)			
(USD-XBT-SEK)	09-05-2014	−0.0581	+0.1211
(GBP-XBT-EUR)	11-07-2014		+0.2148
	13-08-2014		+0.2386
	19-01-2015		−0.0940
	16-04-2015		−0.1100
(RUB-XBT-EUR)	12-02-2015	−0.1377	−0.0908
(USD-XBT-AUD)	08-05-2015		−0.0451

breaks in 2015 leads to less return compared to the benchmark strategy. As for the pairs (USD-XBT-CAD)–(EUR-XBT-GBP) and (USD-XBT-AUD)–(RUB-XBT-EUR), where only some detectors signal a break, the benchmark strategy generates more return for all three breakdates.

5. Summary and Conclusions

We proposed extensions of the monitoring procedures by Wagner and Wied (2017). Again, these extensions are closed-end monitoring procedures designed for a system of cointegrating relationships. Inspired by Chu et al. (1996) we employ parameter estimation over a break-free calibration period and base our procedures on the properly scaled partial sum process while using a functional central limit theorem. We use pooled fully modified OLS estimation in order to construct detectors with nuisance parameter free limiting distributions despite error serial correlation and regressor endogeneity in case of homogeneous parameters and independent cointegrating relations. On the one hand, for dependent cointegrating regressions we utilize a pooled fully modified GLS estimator and on the other hand for dependent and heterogeneous cointegrating regresions we employ the fully modified SUR estimator.

In a simulation study it turns out that the detectors show decent behaviour under the null hypothesis with controlled size and have power against two alternatives under different data generating processes. Self-normalization mitigates the impact of long-run variance estimation on the performance of the detectors based on PFM-OLS estimation. Note that, although no estimator of the long-run variance is necessary in these detector, we

still need one to perform pooled FM-OLS estimation and obtain residuals. The detectors depend on the assumption of homogeneous parameters and independent cointegrating regressions and under violation of these assumptions PFM-GLS and FM-SUR estimation based detectors show proper behaviour under the null hypothesis as well under the alternative hypothesis. Note that a higher number of parameters must be estimated for the detectors based on the latter estimators.

As an illustrative application we test for stability in systems of homogeneous cointegrating relationships in triangular arbitrage parities for logarithmic exchange rate triplets including Bitcoin. We use PFM-OLS based detectors as well as PFM-GLS and FM-SUR detectors for monitoring three different examples of bivariate systems of cointegrating relationships in a sample ranging from 1 May 2013 until 31 December 2015 to see if a stochastic version of the triangular arbitrage parity between currency triplets is stable. In one of the cointegrating relationships almost all detectors indicate breakpoints between May 2014 and April 2015. For the other two cointegrating relationships only a small fraction of detectors indicate breaks. Connected events prior to the detected breaks are the closing of Mt. Gox in February 2014 and the ending of the cap on euro-swiss franc exchange rates by the Swiss National Bank in January 2015. We apply these results to construct a portfolio trading strategy using the detected breaks as a sign of currency market instabilities.

Some extensions to this procedure are conceivable. A better unterstanding of the impact of the weighting function on the performance of the monitoring procedures is still open. Advantages and disadvantages of the detectors regarding power under specicific alternatives could be analyzed in more detail. The multivariate procedures for monitoring cointegration require certain limiting assumptions and relaxing these assumptions for more general applicability is attractive. The self-normalized detectors work better in the multivariate setting and a revisit of the univariate procedure to assess potential improvements is possible. Finally, methods to deal with non-constant variances (especially in financial data) are of great interest.

References

W. Antweiler. Pacific exchange rate service. Sauder School of Business, University of British Columbia, 2015. URL `http://fx.sauder.ubc.ca/`.

A.K. Anundsen. Econometric regime shifts and the us subprime bubble. *Journal of Applied Econometrics*, 30(1):145–169, 2015.

A. Arsova and D.D.K. Örsal. A panel cointegrating rank test with structural breaks and cross-sectional dependence. *Econometrics and Statistics*, 17:107–129, 2021.

Bank of England. United Kingdom: Deposit interest rate. The Global Economy, 2020. URL `https://www.theglobaleconomy.com/United-Kingdom/deposit_interest_rate/`.

Bank of Korea. South Korea: Deposit interest rate. The Global Economy, 2020. URL `https://www.theglobaleconomy.com/South-Korea/deposit_interest_rate/`.

Bitcoincharts. Historic trade data. Bitcoincharts, 2017. URL `http://api.bitcoincharts.com/v1/csv/`.

Board of Governors of the Federal Reserve System. 1-month eurodollar deposit rate London. FRED, Federal Reserve Bank of St. Louis, 2020. URL `https://fred.stlouisfed.org/series/DED1/`.

J. Breitung and M. Pesaran. Unit roots and cointegration in panels. In L. Matyas and P. Sevestre, editors, *The Econometrics of Panel Data: Fundamentals and Recent Developments in Theory and Practice*, chapter 9, pages 279–322. Springer, 2008.

T.S. Breusch and A.R. Pagan. The lagrange multiplier test and its applications to model specification in econometrics. *The Review of Economic Studies*, 47(1):239–253, 1980.

E.-T. Cheah and J. Fry. Speculative bubbles in bitcoin markets? an empirical investigation into the fundamental values of bitcoin. *Economics Letters*, 130:32–36, 2015.

C.-S. J. Chu, M. Stinchcombe, and H. White. Monitoring structural change. *Econometrica*, 64(5):1045–1065, 1996.

S. Corbet, B. Lucey, and L. Yarovaya. Datestamping the bitcoin and ethereum bubbles. *Finance Research Letters*, 26:81–88, 2018.

A. Cretarola and G. Figà-Talamanca. Detecting bubbles in bitcoin price dynamics via *Market Exuberance. Annals of Operations Research*, 299:459–479, 2021.

C. Decker and R. Wattenhofer. Bitcoin transaction malleability and mtgox. In M. Kutyłowski and J. Vaidya, editors, *Computer Security - ESORICS 2014*, pages 313–326. Springer International Publishing, 2014.

H. Dong and W. Dong. Bitcoin: Exchange rate parity, risk premium, and arbitrage stickiness. *British Journal of Economics, Management & Trade*, 5(1):105–113, 2014.

European Money Markets Institute. Euribor. Triami Media B.V., 2020. URL `https://www.euribor-rates.eu/de/euribor-werte-pro-jahr/`.

C. Fink and T. Johann. Bitcoin markets. *SSRN Working Paper (No. 2408396)*, 2014.

M. Jansson. Consistent covariance matrix estimation for linear processes. *Econometric Theory*, 18(6):1449–1459, 2002.

P.S. Lintilhac and A. Tourin. Model-based pairs trading in the bitcoin markets. *Quantitative Finance*, 17(5):703–716, 2017.

H.R. Moon. A note on fully-modified estimation of seemingly unrelated regressions models with integrated regressors. *Economics Letters*, 65:25–31, 1999.

J.Y. Park and M. Ogaki. Seemingly unrelated canonical cointegrating regressions. *Rochester Center for Economic Research: Working Paper No. 280*, 1991.

P. Pasquariello. Financial market dislocations. *Review of Financial Studies*, 27(6):1868–1914, 2014.

P.C.B. Phillips and B.E. Hansen. Statistical inference in instrumental variables regression with i(1) processes. *Review of Economic Studies*, 57(1):99–125, 1990.

P.C.B. Phillips and H.R. Moon. Linear regression limit theory for nonstationary panel data. *Econometrica*, 67(5):1057–1111, 1999.

J. Reynolds, L. Sögner, M. Wagner, and D. Wied. Deviations from triangular arbitrage parity in foreign exchange and bitcoin markets. *TU Dortmund SFB 823 Working Paper 09/18*, 2018.

J. Reynolds, L. Sögner, and M. Wagner. Deviations from triangular arbitrage parity in foreign exchange and bitcoin markets. *Central European Journal of Economic Modelling and Econometrics*, 12(2):105–146, 2021.

Y. Shin. A residual-based test of the null of cointegration against the alternative of no cointegration. *Econometric Theory*, 10(1):91–115, 1994.

T.J. Vogelsang and M. Wagner. Integrated modified ols estimation and fixed-b inference for cointegrating regressions. *Journal of Econometrics*, 178(2):741–760, 2014.

M. Wagner and D. Wied. Consistent monitoring of cointegrating relationships: The us housing market and the subprime crisis. *Journal of Time Series Analysis*, 38(6): 960–980, 2017.

World Bank. Deposit interest rate. The World Bank Group, 2020. URL `https://data.worldbank.org/indicator/FR.INR.DPST/`.

G. Yu and J. Zhang. Revisit capital control policies when bitcoin is in town. *SSRN Working Paper (No. 3053474)*, 2017.

A. Mathematical Appendix

Proof of Lemma 1.
The lemma follows directly from the continuous mapping theorem and our subsequent results Lemma 3, 5 or 7, respectively. $\qquad\square$

Proof of Theorem 1.
For all detectors $\hat{H}_i^{m,+}$, $i = 1, \ldots, 3$ the limits $\mathcal{H}_i^{m,+}$ are well defined under the respective assumptions of Sections 2.1 – 2.3. Analogusly, the limits for $\frac{\hat{H}_i^{m,+}}{g(s)}$ are well defined since $0 < g(s) < \infty$ and $g(s)$ continuous for $0 \le s \le 1$. Therefore, critical values for given $g(s)$ can be found for all versions of the detectors. $\qquad\square$

Proof of Lemma 2:
The result is stated for $\dim D_t = 0$ in Phillips and Moon (1999, p. 1085) in the first equation after (5.16). Using arguments of Phillips and Hansen (1990) it extends easily to the case of arbitrary deterministic trend D_t satisfying Assumption 1. $\qquad\square$

Proof of Lemma 3:
Recall the definition of the N-dimensional PFM-OLS residuals

$$
\begin{aligned}
\hat{u}_{t;m,\text{PFM}}^+ &= y_{t;m,\text{PFM}}^+ - Z_t'\hat{\theta}_{m,\text{PFM}} = y_t - V_t'\hat{\Omega}_{vv;m}^{-1}\hat{\Omega}_{vu;m} - Z_t'\hat{\theta}_{m,\text{PFM}} \\
&= u_t - V_t'\hat{\Omega}_{vv;m}^{-1}\hat{\Omega}_{vu;m} - Z_t'(\hat{\theta}_{m,\text{PFM}} - \theta).
\end{aligned}
\tag{49}
$$

To study the properties of the scaled partial sum process of the PFM-OLS residuals $\left\{ T^{-1/2}\sum_{t=1}^{[sT]} \hat{u}_{t;m,\text{PFM}}^+ \right\}_{s\in[m,1]}$, we consider the decomposition into the above three summands. The limits

$$
T^{-1/2}\sum_{t=1}^{[sT]} u_t \Rightarrow \begin{bmatrix} \omega_{u\cdot v}W_{u\cdot v,1}(s) + \Omega_{uv}\Omega_{vv}^{-1/2}W_{v,1}(s) \\ \vdots \\ \omega_{u\cdot v}W_{u\cdot v,N}(s) + \Omega_{uv}\Omega_{vv}^{-1/2}W_{v,N}(s) \end{bmatrix},
$$

$$
T^{-1/2}\sum_{t=1}^{[sT]} V_t'\hat{\Omega}_{vv;m}^{-1}\hat{\Omega}_{vu;m} \Rightarrow \begin{bmatrix} \Omega_{uv}\Omega_{vv}^{-1/2}W_{v,1}(s) \\ \vdots \\ \Omega_{uv}\Omega_{vv}^{-1/2}W_{v,N}(s) \end{bmatrix}
$$

for $T \to \infty$ are due to Assumption 2 and the consistency of the nonparametric long-run

variance estimators. For the last part, we have

$$
\begin{aligned}
T^{-1/2} \sum_{t=1}^{[sT]} Z_t'(\hat{\theta}_{m,\text{PFM}} - \theta) &= T^{-1/2} \sum_{t=1}^{[sT]} (G_T' Z_t)' G_T^{-1}(\hat{\theta}_{m,\text{PFM}} - \theta) \\
&= \left\{ T^{-1} \sum_{t=1}^{[sT]} \begin{bmatrix} T^{1/2} G_{D,T} D_t & \cdots & T^{1/2} G_{D,T} D_t \\ T^{1/2} X_{1,t} & \cdots & T^{1/2} X_{N,t} \end{bmatrix}' \right\} G_T^{-1}(\hat{\theta}_{m,\text{PFM}} - \theta) \\
&\Rightarrow \omega_{u \cdot v} \int_0^s \mathbf{J}(r)' \mathrm{d}r \left(\sum_{n=1}^{N} \int_0^m J_n(r) J_n(r)' \mathrm{d}r \right)^{-1} \left(\sum_{n=1}^{N} \int_0^m J_n(r) \mathrm{d}W_{u \cdot v,n}(r) \right).
\end{aligned}
$$
(50)

Thus, the asymptotic behaviour of the scaled partial sum process of the PFM-OLS residuals is given by

$$
\begin{aligned}
T^{-1/2} \sum_{t=1}^{[sT]} \hat{u}_{t;m,\text{PFM}}^+ \Rightarrow \omega_{u \cdot v} &\Bigg\{ W_{u \cdot v}(s) - \int_0^s \mathbf{J}(r)' \mathrm{d}r \left(\sum_{n=1}^{N} \int_0^m J_n(r) J_n(r)' \mathrm{d}r \right)^{-1} \\
&\times \left(\sum_{n=1}^{N} \int_0^m J_n(r) \mathrm{d}W_{u \cdot v,n}(r) \right) \Bigg\} = \omega_{u \cdot v} \widehat{W}_{u \cdot v}(s).
\end{aligned}
$$
(51)

$\square$

Proof of Lemma 4:

The proof is similar to the proof of Lemma 2 with an additional transformation typical for generalized least squares estimators, here by the long-run covariance of the modified system error $u_{t;m,\text{GLS}}^+$. $\square$

Proof of Lemma 5:

Besides the incorporation of the generalized least squares transformation, the proof is similar to the proof of Lemma 3. $\square$

Proof of Lemma 6:

This result is stated for $\dim D_t = 0$ in Moon (1999) and is easily extended to the case of arbitrary deterministic trend fulfilling Assumption 1 by arguments of Phillips and Hansen (1990). $\square$

Proof of Lemma 7:

The proof is similar to the proof of Lemma 5. $\square$

B. Simulating Critical Values

Consider the case of Section 2.1. In order to obtain asymptotically size controlled monitoring procedures we need critical values. Therefore, we simulate quantiles of $\sup_{m \leq s \leq 1} \{\frac{\mathcal{H}(s)}{g(s)}\}$, where $\mathcal{H}(s)$ is any of the limiting distribution of the detectors in Lemma 1 and $g(s)$ is the corresponding weighting function (see Table 1). The limiting distributions of the detectors are functionals of the univariate and independent processes

$$
\widehat{W}_{u \cdot v, n}(s) = W_{u \cdot v, n}(s) - \int_0^s J_n(r)' \mathrm{d}r \left(\sum_{j=1}^N \int_0^m J_j(r) J_j(r)' \mathrm{d}r \right)^{-1} \left(\sum_{j=1}^N \int_0^m J_j(r) \mathrm{d}W_{u \cdot v, j}(r) \right)
$$

$n = 1, \ldots, N$ (c.f. (30) and Lemma 3). The processes $\widehat{W}_{u \cdot v, n}(s)$ are functionals of the independent standard Brownian motions $W_{u \cdot v, n}(s)$ and $W_{v, n}(s)$ (recall $J_n(s) = [D(s)', W_{v,n}(s)']'$). We approximate these functionals of standard Brownian motions using the corresponding functions of random walks of length 1,000 generated from i.i.d. standard normal random variables. We justify this by the functional central limit theorem $\mathcal{W}_{v,n}(s) := T^{-1/2} \sum_{j=1}^{[sT]} \mathcal{X}_{j,v,n} \Rightarrow W_{v,n}(s)$ for $T \to \infty$, where $\mathcal{X}_{j,v,n}$ are k-dimensional i.i.d. random vectors with independent standard normal entries and $W_{v,n}(s)$ is a k-dimensional standard Brownian motion. We argue that $T = 1,000$ should be large enough in order for $\mathcal{W}_{v,n}(s)$ to behave approximately like a k-dimensional vector of independent standard Brownian motions. Turning to the three integrals, consider $\int_0^s J_n(r)' \mathrm{d}r = \int_0^s [D(r)', W_{v,n}(r)']' \mathrm{d}r$. Since we know the deterministic function $D(s)$ beforehand we can calculate the integral $\int_0^s D(r)' \mathrm{d}r$ analytically but $\int_0^s W_{v,n}(r)' \mathrm{d}r$ needs to be approximated numerically as well as $\int_0^s J_n(r) J_n(r)' \mathrm{d}r$. Because we have approximated $W_{v,n}(s)$ by a random walk of length 1,000 we take these $1,000m$ (or $1,000s$ in the first integral) discrete points as sampling points for an approximation of the integral by Riemann sums. More precisely, we use $T^{-1} \sum_{r=1}^{[sT]} \mathcal{W}_{v,n}(r/T) = T^{-1} \sum_{r=1}^{[sT]} T^{-1/2} \sum_{j=1}^r \mathcal{X}_{j,v,n} \Rightarrow \int_0^s W_{v,n}(r) \mathrm{d}r$, as $T \to \infty$, and

$$
T^{-1} \sum_{r=1}^{[mT]} \begin{bmatrix} D(r/T) \\ \mathcal{W}_{v,n}(r/T) \end{bmatrix} \begin{bmatrix} D(r/T)' & \mathcal{W}_{v,n}(r/T)' \end{bmatrix} \Rightarrow \int_0^m J_n(r) J_n(r)' \mathrm{d}r,
$$

as $T \to \infty$, and again argue for $T = 1,000$ being large enough for a satisfying approximation. For the third integral define $\mathcal{W}_{u \cdot v, n}(s) := T^{-1/2} \sum_{j=1}^{[sT]} \mathcal{X}_{j,u \cdot v,n}$, where $\mathcal{X}_{j,u \cdot v,n}$ are i.i.d. standard normal random variables. Then, $\mathcal{W}_{u \cdot v, n}(s)$ converges weakly to a standard
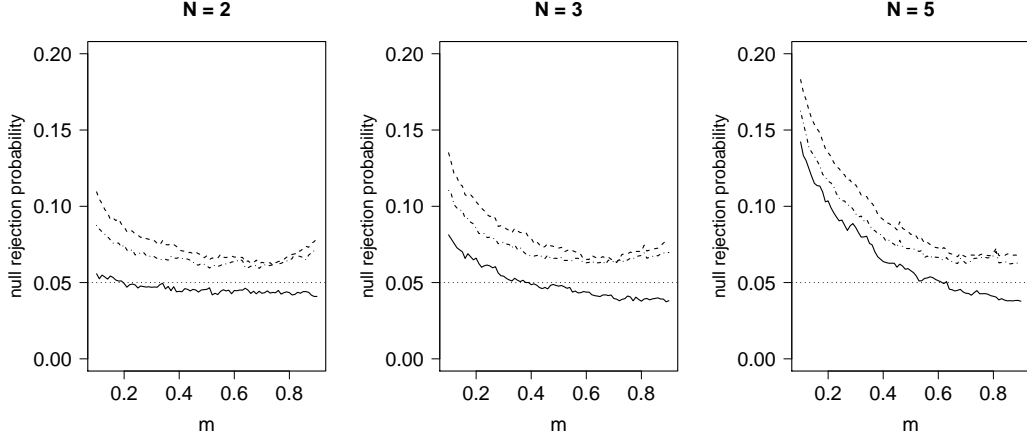
Figure 9: Null rejection probability in correlated homogeneous cointegrating regressions (Section 3.3) with $T = 500$, $\rho_1 = \rho_2 = 0.3$, $\tilde{\rho} = 0.9$ and PFM-OLS estimation. The lines represent $\hat{H}_{1,\text{PFM}}^{m,+}$ (solid), $\hat{H}_{2,\text{PFM}}^{m,+}$ (dashed) and $\hat{H}_{3,\text{PFM}}^{m,+}$ (dotdashed).

Brownian motion $W_{u \cdot v, n}(s)$. By the definition of the Itō-Integral we have

$$\sum_{r=1}^{[mT]} \begin{bmatrix} D((r-1)/T) \\ \mathcal{W}_{v,n}((r-1)/T) \end{bmatrix}' \{\mathcal{W}_{u \cdot v, n}(r/T) - \mathcal{W}_{u \cdot v, n}((r-1)/T)\} \Rightarrow \int_0^m J_n(r) \mathrm{d}W_{u \cdot v, n}(r)$$

for $T \to \infty$. Using numerical integration it is easy to approximate integrals of $\widehat{W}_{u \cdot v, n}(s)$ and hence any of the limiting distributions of the detectors statistics $\mathcal{H}(s)$ by, say, $\mathcal{H}_{\text{approx}}(s)$. Computing $\max_{s=-[mT],\dots,T}\{\frac{\mathcal{H}_{\text{approx}}(s)}{g(s)}\}$ generates one simulated observation. Replicating this 1,000,000 times we approximate the distribution of $\sup_{m \le s \le 1}\{\frac{\mathcal{H}(s)}{g(s)}\}$ and store the $90.0\%, 90.1\%, \dots, 99.9\%$ quantiles.

C. Longrun Covariance and Correlation Matrices

In this section we display the longrun covariance and longrun correlation matrices of the three application examples as well as these of the data generating process used in Section 3.3 and in a robustness check of the detectors based on PFM-OLS against violations of Assumption 4. Figure 9 displays an excerpt of the robustness check for PFM-OLS based detectors and small N. The data generating process is the same as in Section 3.3 for the PFM-GLS and FM-SUR based detectors and the results show that the PFM-OLS based detectors have reaonable empirical size here.

For our choice of $\rho_1 = \rho_2 = 0.3$ and $\tilde{\rho} = 0.9$ the longrun correlation matrix of the errors $\eta_t = [u_{1,t}, u_{2,t}, v_{1,t,1}, v_{1,t,2}, v_{2,t,1}, v_{2,t,2}]'$ in the data generating process (42) and (43) is

$$
\mathrm{Corr}(\eta_t) = \begin{pmatrix}
1.000 & 0.241 & 0.492 & 0.492 & 0.466 & 0.466 \\
0.241 & 1.000 & 0.466 & 0.466 & 0.492 & 0.492 \\
0.492 & 0.466 & 1.000 & 0.900 & 0.900 & 0.900 \\
0.492 & 0.466 & 0.900 & 1.000 & 0.900 & 0.900 \\
0.466 & 0.492 & 0.900 & 0.900 & 1.000 & 0.900 \\
0.466 & 0.492 & 0.900 & 0.900 & 0.900 & 1.000
\end{pmatrix}. \tag{52}
$$

and the estimated longrun correlation matrices in the three application examples are

$$
\widehat{\mathrm{Corr}}(\eta_t) = \begin{pmatrix}
1.000 & 0.508 & 0.074 & -0.093 & 0.088 & -0.074 \\
0.508 & 1.000 & 0.130 & -0.157 & 0.143 & -0.136 \\
0.074 & 0.130 & 1.000 & -0.948 & 0.980 & -0.947 \\
-0.093 & -0.157 & -0.948 & 1.000 & -0.945 & 0.910 \\
0.088 & 0.143 & 0.980 & -0.945 & 1.000 & -0.938 \\
-0.074 & -0.136 & -0.947 & 0.910 & -0.938 & 1.000
\end{pmatrix} \text{ for } \begin{pmatrix} \text{USD-XBT-SEK} \\ \text{EUR-XBT-GBP} \end{pmatrix},
$$

$$
\tag{53}
$$

$$
\widehat{\mathrm{Corr}}(\eta_t) = \begin{pmatrix}
1.000 & 0.818 & -0.039 & -0.010 & -0.041 & 0.016 \\
0.818 & 1.000 & -0.019 & 0.023 & -0.043 & -0.019 \\
-0.039 & -0.019 & 1.000 & -0.926 & 0.900 & -0.965 \\
-0.010 & 0.023 & -0.926 & 1.000 & -0.869 & 0.905 \\
-0.041 & -0.043 & 0.900 & -0.869 & 1.000 & -0.880 \\
0.016 & -0.019 & -0.965 & 0.905 & -0.880 & 1.000
\end{pmatrix} \text{ for } \begin{pmatrix} \text{USD-XBT-CAD} \\ \text{GBP-XBT-EUR} \end{pmatrix},
$$

$$
\tag{54}
$$

and

$$
\widehat{\mathrm{Corr}}(\eta_t) = \begin{pmatrix}
1.000 & 0.768 & 0.018 & 0.037 & -0.052 & 0.011 \\
0.768 & 1.000 & 0.058 & -0.024 & -0.064 & -0.025 \\
0.018 & 0.058 & 1.000 & -0.975 & 0.958 & -0.991 \\
0.037 & -0.024 & -0.975 & 1.000 & -0.961 & 0.976 \\
-0.052 & -0.064 & 0.958 & -0.961 & 1.000 & -0.959 \\
0.011 & -0.025 & -0.991 & 0.976 & -0.959 & 1.000
\end{pmatrix} \text{ for } \begin{pmatrix} \text{USD-XBT-AUD} \\ \text{RUB-XBT-EUR} \end{pmatrix}.
$$

$$
\tag{55}
$$

With a χ^2-test in the style of Breusch and Pagan (1980), it is possible to test for cross-sectional independence of the systems. The null hypothesis is $H_0 : \mathrm{Corr}(u_{1,t}, u_{2,t}) = 0$ and the test statistic is $T_0 \cdot \widehat{\mathrm{Corr}}(u_{1,t}, u_{2,t})$, where $T_0 = 134$ is the length of the calibration sample. The test statistic is asymptotically χ_1^2-distributed under the null hypothesis and in all three cases, the p-value of the test is smaller than 10^{-8}.

The long-run covariance matrix of the errors η_t in the data generating process (42) and

(43) in Section 3.3 for $\rho_1 = \rho_2 = 0.3$ and $\tilde{\rho} = 0.9$ is

$$
\mathrm{Cov}(\eta_t) = \begin{pmatrix}
22.759 & 1.984 & 4.506 & 4.506 & 4.269 & 4.269 \\
1.984 & 22.759 & 4.269 & 4.269 & 4.506 & 4.506 \\
4.506 & 4.269 & 3.063 & 2.756 & 2.756 & 2.756 \\
4.506 & 4.269 & 2.756 & 3.063 & 2.756 & 2.756 \\
4.269 & 4.506 & 2.756 & 2.756 & 3.063 & 2.756 \\
4.269 & 4.506 & 2.756 & 2.756 & 2.756 & 3.063
\end{pmatrix} \times 10^{-3}. \tag{56}
$$

and the estimated long-run covariance matrices in the three application examples are

$$
\widehat{\mathrm{Cov}}(\eta_t) = \begin{pmatrix}
39.803 & 49.693 & 1.076 & -1.389 & 1.293 & -1.108 \\
49.693 & 240.68 & 4.641 & -5.761 & 5.164 & -4.975 \\
1.076 & 4.641 & 5.260 & -5.128 & 5.215 & -5.126 \\
-1.389 & -5.761 & -5.128 & 5.560 & -5.172 & 5.063 \\
1.293 & 5.164 & 5.215 & -5.172 & 5.382 & -5.133 \\
-1.108 & -4.975 & -5.126 & 5.063 & -5.133 & 5.565
\end{pmatrix} \times 10^{-3} \text{ for } \begin{pmatrix} \text{USD-XBT-SEK} \\ \text{EUR-XBT-GBP} \end{pmatrix},
$$

$$\tag{57}$$

$$
\widehat{\mathrm{Cov}}(\eta_t) = \begin{pmatrix}
40.111 & 25.945 & -0.536 & -0.134 & -0.615 & 0.220 \\
25.945 & 25.105 & -0.207 & 0.245 & -0.508 & -0.208 \\
-0.536 & -0.207 & 4.683 & -4.287 & 4.557 & -4.650 \\
-0.134 & 0.245 & -4.287 & 4.574 & -4.349 & 4.313 \\
-0.615 & -0.508 & 4.557 & -4.349 & 5.471 & -4.586 \\
0.220 & -0.208 & -4.650 & 4.313 & -4.586 & 4.961
\end{pmatrix} \times 10^{-3} \text{ for } \begin{pmatrix} \text{USD-XBT-CAD} \\ \text{GBP-XBT-EUR} \end{pmatrix},
$$

$$\tag{58}$$

and

$$
\widehat{\mathrm{Cov}}(\eta_t) = \begin{pmatrix}
28.007 & 83.582 & 0.231 & 0.492 & -0.690 & 0.145 \\
83.582 & 423.098 & 2.995 & -1.222 & -3.301 & -1.255 \\
0.231 & 2.995 & 6.201 & -6.066 & 6.026 & -6.083 \\
0.492 & -1.222 & -6.066 & 6.237 & -6.063 & 6.006 \\
-0.690 & -3.301 & 6.026 & -6.063 & 6.378 & -5.972 \\
0.145 & -1.255 & -6.083 & 6.006 & -5.972 & 6.078
\end{pmatrix} \times 10^{-3} \text{ for } \begin{pmatrix} \text{USD-XBT-AUD} \\ \text{RUB-XBT-EUR} \end{pmatrix}.
$$

$$\tag{59}$$

The difference in estimated long-run variances of $u_{1,t}$ and $u_{2,t}$ in each of the currency triplets (USD-XBT-SEK)-(EUR-XBT-GBP) and (USD-XBT-AUD)-(RUB-XBT-EUR) does not correspond to the simplification proposed in Section 3.3 but the number of estimated parameters remains reasonably low without any simplification as $N = k = 2$ are small.